8-2023

Multiphysics modeling to understand microwave-food interactions in a multi-port solid-state microwave system.

Kartik Verma
University of Tennessee, Knoxville, kverma2@vols.utk.edu

To the Graduate Council:

I am submitting herewith a thesis written by Kartik Verma entitled "Multiphysics modeling to understand microwave-food interactions in a multi-port solid-state microwave system.." I have examined the final electronic copy of this thesis for form and content and recommend that it be accepted in partial fulfillment of the requirements for the degree of Master of Science, with a major in Food Science.

Jiajia Chen, Hao Gan, Major Professor

We have read this thesis and recommend its acceptance:

Mark Morgan, Aly Fathy

Accepted for the Council:
Dixie L. Thompson

Vice Provost and Dean of the Graduate School

(Original signatures are on file with official student records.)

Multiphysics modeling to understand microwave-food interactions in a multi-port solid-state microwave system

A Thesis Presented for the
Master of Science
Degree
The University of Tennessee, Knoxville

Kartik Verma
August 2023

DEDICATION

I dedicate this thesis to my unwavering supporters: my parents, Mr. Sanjay Verma and Mrs. Yogita Verma, my dear sister, Ms. Sumita Verma, my relatives and friends for their love and support throughout this incredible journey.

ACKNOWLEDGMENTS

I am deeply grateful to my esteemed advisors, Dr. Jiajia Chen and Dr. Hao Gan, for their belief in my potential and their opportunity to pursue my master's degree. Their exceptional support and invaluable guidance have played a pivotal role in the successful completion of my project and have prepared me for future endeavors. I extend my heartfelt thanks to them for their patience, dedication, and tireless efforts, which have propelled me to succ in my master's program. Their mentorship has left an indelible mark on my professional growth, and I will forever carry a profound sense of gratitude toward them.

I would also like to express my profound appreciation to my esteemed committee members, Dr. Mark Morgan, and Dr. Aly Fathy, for their invaluable assistance and for sharing their knowledge with me throughout my project. Their wisdom, guidance, and knowledge have been instrumental in shaping my research and refining my academic skills. I am genuinely grateful for their expertise and commitment to my success.

Furthermore, I extend my sincere acknowledgment and gratitude to all the members of my lab and my peers in the Food Science Department at the University of Tennessee, Knoxville. Their collaboration, camaraderie, and knowledge-sharing environment have created a fertile ground for personal and intellectual growth.

I would also like to express my deepest gratitude to my friends in both Knoxville and India. Their unwavering motivation, encouragement, and belief in my abilities have been a constant

source of inspiration throughout my career. Their support and insightful advice have been invaluable in shaping my path, and I am forever indebted to them.

Last but certainly not least, I want to express my gratitude to my parents and family. Their unconditional love, trust, and support from afar have been immeasurable. I am deeply grateful for their sacrifices, belief in my abilities, and constant encouragement. Their faith in me has been a driving force behind my accomplishments. I also want to thank the almighty for providing me with a strong support system throughout my journey.

Once again, I want to extend my deepest appreciation to everyone who has contributed to my academic and personal growth. Th support, encouragement, and guidance I have received along the way have been remarkable. I am forever grateful for the opportunities and the transformative experiences that have shaped me into who I am today.

ABSTRACT

Multiphysics modeling plays a crucial role in understanding the complexities of microwave-food interactions, especially in multi-port solid-state microwave systems where microwave parameters can be precisely and dynamically controlled. However, previous models using simplistic or manually measured oven geometries face challenges in accurately simulating the microwave heating process. This study first developed a robust 3-D scanning approach to capture precise geometric details of the oven cavity, incorporating them into multiphysics modeling for solid-state microwave heating. Furthermore, a quantitative validation approach was also developed to characterize modeling accuracy against experimental results. The results showed that multiphysics modeling with 3-D scanned geometry demonstrated improved prediction accuracy, with notably lower root mean square error (RMSE) values (ranging from 1.57 to 4.11 °C) compared to models using simple box geometry (ranging from 1.73 to 6.33 °C) and manually measured geometry (ranging from 1.48 to 4.66 °C) for various heating scenarios with various frequencies (2.40, 2.45, and 2.48 GHz) and waveguide port locations (Right, Back, and Left).

The study further focuses on utilizing the multi-port solid-state microwave heating processes and investigates the impact of differential phase between multiple sources on microwave-food interactions. To improve the modeling efficiency in simulating extensive scenarios of relative phase (0° to 360°), this study developed a simple analytical approach that extends the existing knowledge of plane wave interactions to encompass multi-mode standing wave interactions. By employing only four physics-based models, this analytical approach enables the prediction of microwave power densities at any arbitrary source phase difference ranging from 0° to 360°.To validate the performance of the developed analytical model, comparisons were made with results

obtained from the physics-based models in terms of electric field and power dissipation densities. After validation, extensive predictions and characterizations of differential phase-dependent microwave power densities revealed wave-like patterns in the average, standard deviation, and coefficient of variations of the nodal power densities. This observation emphasizes the importance of selecting an appropriate differential phase to ensure uniform heating performance.

The developed 3-D scanning approach, improved multiphysics model, and simple analytical model provide useful tools to evaluate complicated microwave-food interactions to develop solid-state microwave processing technology.

TABLE OF CONTENTS

LIST OF TABLES

LIST OF FIGURES

CHAPTER I: INTRODUCTION AND BACKGROUND

1.1 Introduction

Microwave ovens are incredibly popular and widely used in households due to their rapid heating, user-friendly operation, and high level of convenience (Pitchai et al. 2016; Yang and Chen 2021). The food product in a domestic microwave oven undergoes heating through the polarization effect of electromagnetic radiation operating at a frequency of 2.45 GHz. This microwave energy effectively permeates the outer layer of the food, resulting in localized heating because of molecular friction arising from the dipolar rotation of polar solvents, specifically water molecules contained within the food (He et al. 2020). With their versatility and various advantages, such as rapid heating, thorough cooking, efficient energy absorption, reduced cooking time, and overall convenience, microwave ovens have been embraced by 95% of households in the United States (Yang and Chen 2021). The microwave oven market in the U.S. alone was valued at over $7 billion in 2020, experiencing a Compound Annual Growth Rate (CAGR) of 4.18%. It is projected to further increase to 4.72% between 2022 and 2026. By 2024, the global market for microwave ovens and microwavable food products is expected to surpass $142 billion (Yang 2022).

Despite its many benefits, the microwave heating process has a significant drawback, i.e., non-uniform heating. The problem arises from formation of a standing wave pattern inside the microwave oven, which creates hot and cold spots in the food, leading to food quality and safety issues, respectively (Vadivambal and Jayas 2010; Kamol et al. 2010; Guzik et al. 2022). Both oven and food factors contribute to the non-uniform heating issue. For the multimode microwave oven cavity, the electric field is not uniformly distributed inside the oven cavity, and a standing wave pattern is generated, resulting in nonuniform heating within the food products. The

dielectric properties of food products change with temperature during the heating process, causing a thermal runaway effect where hot spots absorb more energy and thus are heated more than the cold spots(Akkari et al. 2006; Atuonwu and Tassou 2018). The magnetron also cannot generate a stable microwave in a stable manner, which also influences the microwave heating process. For example, in recent research, it has been observed that magnetrons emit microwave radiation covering a wide frequency range, extending up to 70 MHz which depends on the specific location of the food within the oven and the type of food being heated (Luan et al. 2017; Zhou, Pedrow, et al. 2023). Addressing these challenges is crucial to ensure consistent and reliable microwave heating that preserves the food's quality and safety.

Various techniques have been employed in modern microwave ovens to achieve uniformity in microwave heating. These include rotating turntables and mode stirrers, disrupting the fixed thermal pattern and electric field distribution within the oven cavity leading to better uniformity(Plaza-González et al. 2005; Geedipalli et al. 2007). Additionally, operational strategies such as intermittent heating, multiple power sources, frequency shifting heating, and power level control are implemented to enhance the microwave heating process. These methods, along with other process control approaches, contribute to improving overall performance (Atuonwu and Tassou 2018).

A notable advancement in this regard is the solid-state microwave generator, which combines all these improvements into a single system and can potentially improve the microwave heating process by disturbing the standing wave pattern (Yang and Chen, 2022). The research and development in the semiconductor industry have led to the emergence, improvement, and

adoption of solid-state microwave generators as a potential replacement for traditional magnetron-based systems. Compared to magnetrons, semiconductor-based solid-state generators provide longer lifetimes, stable control over frequency, multiple sources with independent control, accessibility to feedback and process optimization algorithms, precise control over power and relative phase, lower operational voltages, and better adaptability to electronic circuits(Atuonwu and Tassou 2018; Chaudhry et al. 2019; Zhou, Pedrow, et al. 2023).

Another significant advantage due to the small size of solid-state devices is the possibility of multi-source operations with independent control of power, phase, and frequency, providing ample opportunities for process optimization (Bows et al. 1999a; Przemyslaw Korpas, Krysicki, et al. 2014). Unlike the lack of control of operational parameters in conventional microwave ovens, which are usually equipped with a single microwave source, solid-state microwave ovens offer control over individual or combined amplitude and phase, allowing directed energy levels to specific areas. This approach eliminates the need for turntables and stirrers, resulting in more even heat distribution and additional power control (Handinger 2004; Chaudhry et al. 2019). The multiple-port configuration offers greater flexibility in controlling the heating process, as different food products may require specific energy distributions for optimal results.

The relative phase between the multiple independently controlled sources plays a crucial role in the performance and uniformity of microwave heating in multi-source solid-state microwave ovens such that the waves can be displaced in time to change the electric field patterns inside the oven cavity and food product(Wang et al. 2021; Ahn et al. 2023). These waves from multiple sources having a relative phase difference interfere with each other, leading to constructive or

destructive interference patterns, depending on the relative phase between the sources. Constructive interference occurs when the waves from different sources are in phase, meaning their peaks and troughs align (Bows et al. 1999a). This reinforces the electric field, leading to higher energy levels at specific locations in the oven cavity. On the other hand, destructive interference occurs when the waves are out of phase, causing cancellation or reduction of the electric field intensity at certain positions. By carefully adjusting the relative phase between the microwave sources, it is possible to achieve constructive interference in desired areas and destructive interference in undesired regions. This control over the interference patterns allows for manipulating energy distribution and enables more uniform heating of the food product (Korpas et al. 2014; Wang et al. 2021; Ahn et al. 2023).

Studying the interactions among food, packaging, and microwaves can be challenging when conducted experimentally, primarily due to the intricate physics and multiple factors involved in the microwave heating process. The involvement of numerous factors, such as properties and shape of the food product, microwave frequency, and oven design, adds to the complexities and makes it difficult to observe and understand these interactions through experiments alone (Pitchai et al. 2014). Mathematical modeling is a promising tool to better understand and optimize the microwave heating process. Modeling of microwave heating process helps in simulating and analyzing the complex interactions involved, enhances the understanding of the microwave-food interaction, and assists in designing better food products and packages (Zhang and Datta, 2000; Geedipalli et al., 2008; Chen et al., 2014). Also, it becomes more crucial in the solid-state microwave heating process as various operational parameters can be controlled precisely, leading to more complicated microwave-food interaction.

Before applying multiphysics-based models for developing microwaveable foods with enhanced uniformity and improved heating, it is essential to validate these models' accuracy. Hence, the development of a robust multiphysics-based model that can accurately predict both hot and cold spots, as well as provide an accurate temperature distribution, becomes highly significant. Nevertheless, there are still notable challenges in developing robust computer simulations with high prediction accuracy, which has resulted in some reservations regarding the widespread adoption of microwave heating processes in the industry.

Therefore, this thesis focuses on developing a robust model for a multi-source solid-state microwave oven and validating its prediction accuracy. To simulate and create a reliable model for the microwave heating process, the geometry of the microwave oven plays a significant role. Typically, microwave oven cavities feature irregular major and minor protrusions on their walls, strategically designed to concentrate the microwave energy in specific areas and enhance power absorption and heating performance. However, early models often overlooked these protrusions, employing simple cuboidal cavities, which made it challenging to accurately predict heating patterns and temperature distribution (Geedipalli et al., 2007; Pitchai et al., 2012; Su et al., 2022). With technological advancements, researchers started adding these protrusions into their work by measuring them manually. While this inclusion improved the process, there was still room for further enhancement (Chen F. et al. 2016; Gulati et al. 2016).

Therefore, this study utilizes 3-D scanning technology to capture the precise geometric details of the oven cavity at a high resolution, up to 0.1 mm. By employing 3-D scanning, both minor and

major protrusions can be accurately captured, overcoming the challenges associated with manual measurements. Previous studies have also demonstrated the effectiveness of 3-D scanning technology in capturing irregular geometries accurately (Kim et al., 2007; Kuffi et al., 2016; Zhang et al., 2020). Furthermore, the current models commonly rely on qualitative validation of the microwave heating process, using terms such as "good agreement" or "generally matching" between experimental and simulation results (Pitchai et al. 2016; Zhou, Pedrow, et al. 2023). However, a more robust validation approach is crucial. Therefore, this thesis adopts a quantitative validation approach to enhance the validation of the microwave heating process. The quantitative approach involves comparing the pixel temperature differences between the simulation and experimental heating results and calculating the root mean square error (RMSE) value. By comparing these RMSE values, a more comprehensive and reliable validation can be achieved.

Once the robust multiphysics models have been developed and validated, they can be utilized to investigate the interaction between multiple ports and characterize the multi-source solid-state microwave heating process. The developed model enables simulation of the microwave heating process at various relative phase values in the solid-state microwave heating process to improve uniformity. Therefore, the third chapter of this thesis uses the validated model to simulate the multiple-port interactions and study the effect of relative phases on heating uniformity.

Solid-state generators have the capability to precisely adjust the relative phase, with a step size of 1° covering the entire 0° to 360° range. Studies on phase manipulation have demonstrated the effectiveness of optimizing the relative phase in improving the uniformity of food products in

solid-state microwave systems (Wang et al. 2021; Ahn et al. 2023). However, current modeling approaches only simulate the microwave heating process at specific relative phase values, failing to utilize the full range and limiting the potential for optimizing the microwave heating process.

Microwave engineering has extensively investigated interactions among multiple plane microwaves, providing valuable insights into multi-port interactions within solid-state microwave heating processes (Bows et al. 1999a; Korpas et al. 2014) . Nonetheless, simulating the microwave heating process at each step size can be time-consuming and computationally demanding. For example, when simulating the microwave heating process in a solid-state microwave system with a particular relative phase value, it typically requires around 10-15 minutes of computational time on a computer system equipped with two 16-core Intel(R) Xeon(R) processors equipped with 3.20 GHz wavenumber and accompanied by 128 GB of RAM. The system runs on the Windows 10 operating system. Moreover, analyzing the thermal pattern and heating uniformity requires additional time and computational resources, making it challenging to determine the optimal values for the microwave heating process.

This study proposes a simple analytical model to address these limitations and leverage the knowledge gained from interactions among multiple plane waves. By drawing insights from a minimal number of physics-based modeling studies, this thesis aims to capture the interactions accurately and efficiently among multiple ports with different relative phases in solid-state microwave heating systems. This analytical model will contribute to our understanding of the interactions between multiple sources while facilitating the optimization of microwave heating processes.

Therefore, to achieve the overall objective of using the multi-source solid-state microwave oven to heat the food product at a desired area selectively, this project is composed of two specific objectives, which are:

Objective 1: Development and validation of a robust and expandable Multiphysics-based model for multi-source solid-state microwave system.

Objective 2: Development of a simple and accurate analytical model to understand the effect of relative phase in a dual-port solid-state microwave heating process.

References

Ahn, S.H., Jeong, C.H., Lee, W.S., 2023. 0.5kWatt 2.45 GHz GaN-based microwave heating system design with active phase control. Microw Opt Technol Lett. https://doi.org/10.1002/mop.33689

Akkari, E., Chevallier, S., Boillereaux, L., 2006. Observer-based monitoring of thermal runaway in microwaves food defrosting. J Process Control 16, 993–1001. https://doi.org/10.1016/j.jprocont.2006.05.005

Atuonwu, J.C., Tassou, S.A., 2018. Quality assurance in microwave food processing and the enabling potentials of solid-state power generators: A review. J Food Eng. https://doi.org/10.1016/j.jfoodeng.2018.04.009

Bows, J.R., Patrick, M.L., Janes, R., Ricky' Metaxas, A.C.', Dibben, D.C., 1999. Microwave phase control heating. Int J Food Sci Technol 34, 295–304.

Chaudhry, K.A., Eng, B., Hons, P.-F., 2019. Solid-State Technology for Domestic Microwave Heating Applications.

Chen, F., Warning, A.D., Datta, A.K., Chen, X., 2016. Thawing in a microwave cavity: Comprehensive understanding of inverter and cycled heating. J Food Eng 180, 87–100. https://doi.org/10.1016/j.jfoodeng.2016.02.007

Chen, J., Pitchai, K., Birla, S., Negahban, M., Jones, D., Subbiah, J., 2014. Heat and mass transport during microwave heating of mashed potato in domestic oven-model development, validation, and sensitivity analysis. J Food Sci 79, E1991–E2004. https://doi.org/10.1111/1750-3841.12636

Geedipalli, S., Datta, A.K., Rakesh, V., 2008. Heat transfer in a combination microwave-jet impingement oven. Food Bioprod Process 86, 53–63. https://doi.org/10.1016/j.fbp.2007.10.016

Geedipalli, S.S.R., Rakesh, V., Datta, A.K., 2007. Modeling the heating uniformity contributed by a rotating turntable in microwave ovens. J Food Eng 82, 359–368. https://doi.org/10.1016/j.jfoodeng.2007.02.050

Gulati, T., Zhu, H., Datta, A.K., 2016. Coupled electromagnetics, multiphase transport and large deformation model for microwave drying. Chem Eng Sci 156, 206–228. https://doi.org/10.1016/j.ces.2016.09.004

Guzik, P., Kulawik, P., Zając, M., Migdał, W., 2022. Microwave applications in the food industry: an overview of recent developments. Crit Rev Food Sci Nutr. https://doi.org/10.1080/10408398.2021.1922871

Handinger, P., 2004. Microwave heating using distributed semiconductor sources.

He, J., Yang, Y., Zhu, H., Li, K., Yao, W., Huang, K., 2020. Microwave heating based on two rotary waveguides to improve efficiency and uniformity by gradient descent method. Appl Therm Eng 178. https://doi.org/10.1016/j.applthermaleng.2020.115594

Kamol, S., Limsuwan, P., Onreabroy, W., 2010. Three-dimensional standing waves in a microwave oven. Am J Phys 78, 492–495. https://doi.org/10.1119/1.3329286

Korpas, Przemyslaw, Krysicki, M., Więckowski, A., 2014. Phase-Shift-Based Efficiency Optimization in Microwave Processing of Materials with Solid-State Sources. 16th Seminar Computer Modeling in Microwave Power Engineering, Karlsruhe, Germany, May 12-13, 2014.

Luan, D., Wang, Y., Tang, J., Jain, D., 2017. Frequency Distribution in Domestic Microwave Ovens and Its Influence on Heating Pattern. J Food Sci 82, 429–436. https://doi.org/10.1111/1750-3841.13587

Pitchai, K., Chen, J., Birla, S., Gonzalez, R., Jones, D., Subbiah, J., 2014. A microwave heat transfer model for a rotating multi-component meal in a domestic oven: Development and validation. J Food Eng 128, 60–71. https://doi.org/10.1016/j.jfoodeng.2013.12.015

Pitchai, K., Chen, J., Birla, S., Jones, D., Subbiah, J., 2016. Modeling microwave heating of frozen mashed potato in a domestic oven incorporating electromagnetic frequency spectrum. J Food Eng 173, 124–131. https://doi.org/10.1016/j.jfoodeng.2015.11.002

Plaza-González, P., Monzó-Cabrera, J., Catalá-Civera, J.M., Sánchez-Hernández, D., 2005. Effect of mode-stirrer configurations on dielectric heating performance in multimode microwave applicators. IEEE Trans Microw Theory Tech 53, 1699–1705. https://doi.org/10.1109/TMTT.2005.847066

Vadivambal, R., Jayas, D.S., 2010. Non-uniform temperature distribution during microwave heating of food materials-A review. Food Bioproc Tech. https://doi.org/10.1007/s11947-008-0136-0

Wang, C., Yao, W., Zhu, H., Yang, Y., Yan, L., 2021. Uniform and highly efficient microwave heating based on dual-port phase-difference-shifting method. Int. J. RF Microw. Comput.-Aided Eng 31. https://doi.org/10.1002/mmce.22784

Yang R. 2022. Microwave Frequency Control Algorithms for Use in a Solid-State Microwave Frequency Control Algorithms for Use in a Solid-State System to Achieve Improved Heating Performance System to Achieve Improved Heating Performance. https://trace.tennessee.edu/utk_graddiss

Yang, R., Chen, J., 2022. Dynamic solid-state microwave defrosting strategy with shifting frequency and adaptive power improves thawing performance. Innov Food Sci Emerg Technol 81. https://doi.org/10.1016/j.ifset.2022.103157

Yang, R., Chen, J., 2021. Mechanistic and machine learning modeling of microwave heating process in domestic ovens: A review. Foods 10. https://doi.org/10.3390/foods10092029

Zhang, H., Datta, A.K., 2000. Coupled electromagnetic and thermal modeling of microwave oven heating of foods. J Microw Power Electromagn Energy 35, 71–85. https://doi.org/10.1080/08327823.2000.11688421

Zhang, R., Li, F., Tang, J., Koral, T., Jiao, Y., 2020. Improved accuracy of radio frequency (RF) heating simulations using 3D scanning techniques for irregular-shape food. LWT- Food Sci Technol 121. https://doi.org/10.1016/j.lwt.2019.108951

Zhou, X., Pedrow, P.D., Tang, Z., Bohnet, S., Sablani, S.S., Tang, J., 2023. Heating performance of microwave ovens powered by magnetron and solid-state generators. Innov Food Sci Emerg Technol 83. https://doi.org/10.1016/j.ifset.2022.103240

CHAPTER II: 3-D SCANNED OVEN GEOMETRY IMPROVES THE MODELING ACCURACY OF THE SOLID-STATE MICROWAVE HEATING PROCESS

A version of this chapter has been submitted to the Journal of Microwave Power and Electromagnetic Energy and is under review.

Verma K, Nachtab J, Dvorak J, Alley P, Yang R, Gan H, Chen J. “3-D Scanned oven geometry improves the modeling accuracy of the solid-state microwave heating process.” Journal of Microwave Power and Electromagnetic Energy (2023)

2.1 Abstract

Solid-state-based microwave ovens are considered a potential replacement to the current magnetron-based microwave ovens to mitigate the non-uniformity issue for their precise control over microwave parameters. Multiphysics modeling is a useful tool for understanding complicated microwave heating processes. However, previous models using simple or manually measured oven geometry had challenges in accurately predicting the heating patterns. This study developed a 3-D scanning approach to characterize the accurate geometric details of the cavity and incorporate it in the multiphysics modeling of solid-state microwave heating. The effect of oven geometric details on modeling accuracy was evaluated for models using the simple box, manually measured, and 3-D scanned geometries at multiple microwave frequencies and port locations. A quantitative approach to compare the RMSE values between the simulation and experiments was also developed to replace the previously often-used qualitative approach to compare the spatial temperature profiles between the simulation and experiments. The Multiphysics-based models using 3-D scanned geometry showed significantly or considerably smaller RMSE values (1.57 to 4.11 °C) than the models with simple box geometry (1.73 to 6.33 °C) and manually measured geometry (1.48 to 4.66 °C) at most heating scenarios with multiple frequencies (2.40, 2.45, and 2.48 GHz) and waveguide port locations (Right, Back, and Left).

The 3-D scanned approach can accurately incorporate the irregular geometric details of the oven cavity and can improve the prediction accuracy of microwave heating models. The robust models for the solid-state microwave systems using 3-D scanned geometries can be used in understanding microwave-food interactions in multisource solid-state microwave heating processes.

2.2 Keywords

Solid-state, 3-D scanning, thermal images, heating pattern, simulation, COMSOL

2.3 Introduction

Non-uniform heating remains one of the biggest concerns of microwave-heated foods, which not only causes the thermal deterioration of the food product at hot spots but also leads to potential food safety issues at the cold spots (He et al. 2020; Yang and Chen 2021). Microwave heating is a complex process due to the complicated interactions between microwaves and food products, where many factors are involved, such as food composition, food properties (thermal and dielectric properties), container shape, oven geometry, and food location. Multiphysics modeling has been used as a valuable tool to study the microwave heating process, enhance the understanding of microwave-food interactions, and assist food product developers in designing better microwaveable foods. It is more important in the solid-state microwave heating processes because microwave parameters of frequencies, powers, and relative phases (for multiple ports) can be precisely controlled, resulting in more complicated microwave-food interactions.

Validating the accuracy of the multiphysics-based models before use is essential for food developers to propose solutions to the non-uniformity issues in the designed microwaveable foods. For example, the models can be first used to predict the temperature distributions and hot/cold spot

locations within the heated products, and then shield packages can be designed to prevent the overheating of these hot spots (Perry and Lentz 2021). However, developing robust computer simulations with high prediction accuracy still has significant challenges.

The microwave oven geometry is one parameter that significantly influences the microwave heating results due to the back-and-forth reflections of the microwave at cavity walls. The microwave oven cavity often has irregular major and minor protrusions on the walls, specifically designed to improve microwave power absorption and heating performance. However, due to the limited computational resources, early-stage microwave heating models usually used simple cuboidal boxes to represent the oven cavity (Geedipalli et al. 2007; Pitchai et al. 2012; Su et al. 2022), making it challenging to predict the heating patterns accurately. Later studies incorporated more geometric details of the oven cavity in the models by manually measuring major protrusions of the oven walls (Chen F. et al. 2016; Gulati et al. 2016). Although the accuracy of the predicted heating patterns was improved, the geometric details (e.g., the minor protrusions and curvatures of the oven cavity) still need to be included in the models to improve the prediction accuracy further.

Moreover, a robust quantitative validation approach is critically needed to validate the microwave heating models. Temperature distributions at food surfaces captured by thermal imaging cameras have been widely used in validating the modeling of microwave and radiofrequency heating processes. Some quantitative comparison approaches, such as average and standard deviation of the spatial temperature and difference between maximum and minimum temperatures, were used in the validation discussion, especially for radiofrequency processes(Wang et al. 2005; Alfaifi et al. 2014; Jiao et al. 2014; Huang et al. 2018). However, these validation approaches were not widely used or robust enough in validating microwave heating models. Current microwave heating

model validation on heating patterns often uses a qualitative approach, where "good agreement" or "generally match" are often used in describing the comparison between simulation and experiments. Domestic microwave heating process is complicated due the multimode cavity of microwave ovens and temperature-dependent dielectric properties of food products. The validation based on average temperature and/or temperature difference or any experimental conditions (e.g., rotation of turntable) that cause averaging effect on heating patterns cannot robustly validate the accuracy of the microwave heating models. Therefore, a quantitative approach is critically needed to compare the simulated and experimental heating patterns.

Three-dimensional (3-D) scanning technology is promising to capture geometric details in a high resolution, i.e., up to 0.1 mm. The 3-D scanning approach has been used to capture accurate geometries of the food products having irregular shapes to improve modeling accuracy. Uyar and Erdoğdu, (2009) studied the effectiveness of using a 3-D scanner to obtain accurate geometric details of pears, strawberries, bananas, apples, and eggs. Compared to the actual measurement, the predicted diameter, surface area, and volume errors were less than 1%, demonstrating the efficiency and precision of 3-D scanning. Multiple other studies emphasized the need to accurately capture the geometric details of the food products to model the food preservation processes precisely (Kim et al. 2007; Kuffi et al. 2016). Kuffi et al. (2016) developed a computational fluid dynamics (CFD) model to predict the temperature and pH changes in the beef carcass during the chilling process. A 3-D scanned geometry of the carcass obtained from a high-resolution 3-D laser scanning system was used in the model. The results obtained from the simulations were in good agreement with the experimental results attributed to the detailed 3-D geometry of the carcass. R. Zhang et al. (2020) used the 3-D scanning approach to scan the irregular geometry of potato, carrots, and ginger root food products. These irregular geometries were created with CAD software

and eventually imported into finite element method software (i.e., COMSOL) for the RF heating simulations. The models using 3-D scanned geometry showed improved temperature prediction accuracy than those using regular-shaped geometry (from ~91% to ~95%) based on seven predefined locations, which showed the great potential of the 3-D scanning approach. The successes in applying 3-D scanned geometry to improve modeling accuracy indicate the potential of enhancing microwave modeling accuracy using 3-D scanning technology.

The objectives of this study were to:

(1) to develop a 3-D scanning approach to characterize the oven cavity geometry for modeling the solid-state microwave heating process;
(2) to develop a quantitative approach to evaluate the modeling accuracy of the heating patterns;
(3) to compare the modeling accuracy among models using simple-box, manually measured, and 3-D scanned oven cavity geometries.

2.4 Materials and Methods

2.4.1 Model Development

2.4.1.1 Microwave system and model geometry

A fabricated multiport solid-state microwave system was used in this study. The microwave system was composed of a solid-state microwave generator (PA-2400-2500 MHz-200 W-4, Junze Technology, China), four coaxial cables connected to four waveguides (CWR340 CentricRF) through four launcher ports, and a commercial microwave oven cavity (Panasonic Model NN-SN936W) without the original magneton or waveguide, as shown in Figure 2.1. The multiport solid-state microwave system can accurately control the microwave frequency up to

0.1 MHz between 2.40 and 2.50 GHz up to 0.1 MHz (Zhou et al. 2023), minimizing the effect of frequency variation on heating patterns. In addition, the available multiport and multiple frequencies also enable a comprehensive validation of the heating pattern accuracy.

Since the overall goal of this study was to evaluate the effect of oven cavity geometric details on the simulation accuracy, three different geometric models (simple box, manually measured, and 3-D scanned) with various cavity details were characterized and used in the multiphysics modeling, as shown in Figure 2.2. In addition, the geometries of the turntable, food product, and four waveguides were also included in the three geometric models. The geometry of the plastic container (made from polypropylene) was ignored in the geometry due to its low dielectric properties and thin layer, making it a transparent material to the microwave.

The simple box geometry was developed by considering the oven cavity as a rectangular box using the main dimensions (length, width, and height) of the oven cavity, as shown in Figure 2.2(A). The geometric details of major and minor protrusions on the cavity walls were not captured or included in the simple box geometry. The manually measured geometry was characterized by manually measuring the major protrusions on the left, right, back, front, top, and bottom walls using a handheld caliper, as shown in Figure 2.2(B). In this geometry, the minor protrusions from the right, back, and bottom faces were not characterized as these minor protrusions were very thin to be manually measured. The simple box and manually measured geometry were created using the available geometry function in COMSOL Multiphysics v6.0 (COMSOL Inc., Boston, MA).

The 3-D scanned geometry was characterized by a 3-D scanning approach to obtain an accurate geometry, as shown in Figure 2.2(C). Three steps of scanning, meshing, and generating solid geometry were used to create the detailed oven cavity geometry, as shown in Figure 2.3. First, ~ 100 circular black and white scanning targets having a diameter of 3 mm were placed inside the

cavity and used as scanning reference points (Sihu Future Technology co., Ltd), as shown in Figure 2.3(A). A handheld structured light Artec-3-D scanner (Artec EVA-S, Artec) with a maximum accuracy of 0.1mm was panned and tilted inside the cavity to generate a point cloud of the cavity (Figure 2.3A). Each oven cavity wall was captured individually to ensure high resolution and aligned based on the scanning targets in the Artec software. Then, the formed point cloud was converted into a mesh (Figure 2.3B) and imported into the Geomagic Design X software (Geomagic® Design X ™, Oqton, San Francisco, CA). The imported mesh was run through an automatic diagnostic tool known as healing wizard to find and solve any mismatching discrepancies. Finally, the cleaned mesh was converted into a solid geometry using the auto surface option in Geomagic (Figure 2.3C). The glass turntable forms an essential part of the oven geometry, and due to its irregular geometry, it can be difficult to build manually. In order to accurately capture the glass turntable, identical steps mentioned above were performed to obtain the scanned geometry for the turntable, as shown in Figure 2.4. The solid geometry for the oven cavity and glass turntable was then exported as a STEP file that can be imported into the COMSOL Multiphysics software using the CAD import module. The final geometry is comprised of the scanned oven cavity with major and minor details, along with the glass turntable.

2.4.1.2 Governing equations

The physics of electromagnetics and heat transfer were used in the models to simulate the microwave heating process.

To solve the electromagnetic field distribution inside the oven cavity, Maxwell's waveform equations are used (Chen J. et al. 2016):

$$\nabla \times \mu_r^{-1}\left(\nabla \times \vec{E}\right) - \left(\frac{2\pi f}{c}\right)^2(\varepsilon' - j\varepsilon'')\vec{E} = 0 \quad (1)$$

where, ε'refers to the dielectric constant, $\varepsilon''$is the dielectric loss factor, μ_r is the electromagnetic permeability of the food product, f is the microwave frequency in Hz, $\vec{E}$ refers to the electric field intensity in V/m, c is the speed of light in m/s, and j is $\sqrt{-1}$.

Fourier's heat transfer equation was used to describe the heat transfer process in the food product:

$$\rho C_P \frac{\partial T}{\partial t} = \nabla \cdot (k \nabla T) + P \qquad (2)$$

This equation takes into account parameters including density (ρ, kg/m^3), specific heat (Cp, J/kg.K), temperature (T, °C), thermal conductivity (k, W/m.K), and the dissipated microwave power density acting as the heat source (P, W/m^3).

The dissipated power density (P, W/m^3) is described as:

$$P = \pi \varepsilon_0 \varepsilon'' f |\vec{E}|^2 \qquad (3)$$

where, ε_0 refers to free space permittivity and has a value of 8.854×10^{-12} F m^{-1}, $\varepsilon''$is the dielectric loss factor, f is the microwave frequency in Hz, and $\vec{E}$ refers to the electric field intensity in V/m.

2.4.1.3 Boundary and initial conditions

The boundary conditions in the electromagnetics were set such that the walls were considered to be perfect electric conductors, ensuring that the tangential component of the electric field is zero. This boundary condition accurately models the lossless metallic surface of the walls.

$$n \times \vec{E} = 0 \qquad (4)$$

where, n is the normal vector.

At the surface of the food product, convective heat transfer between the food product and the surrounding air was described as:

$$-k \frac{\partial T}{\partial \vec{n}} = h(T - T_{ext}) \qquad (5)$$

where h (W/m^2K) is the convective heat flux and is assumed to be constant (10 W/m^2K) for the entire microwave heating process, and T_{ext} (°C) is the temperature of surrounding air which was assumed as a constant value of 25 °C.

The initial temperature of the food product of 4 °C was used in all the models.

2.4.1.4 Material properties

The physical, dielectric, and/or thermal properties of air, glass (turntable), and mashed potato (food) were obtained from the literature and/or the COMSOL material library and applied in corresponding domains, as summarized in Table 2.1.

2.4.1.5 Meshing strategy

The tetrahedral mesh was used in generating the mesh. A mesh-independent study was performed following the procedures described in (Chen et al. 2014) which studied the effect of mesh refinement on the normalized power absorption. The maximum element sizes of the air domain (15 mm), turntable (5 mm), and food product (3 mm) were identified as suitable for models with different oven geometry types. The mesh for the different domains (food product, turntable, and oven cavity) and geometries (simple box, manually measured, and 3-D scanned geometry) are shown in Figure 2.5. As observed, the mesh of the 3-D scanned geometry showed much finer meshes than the other two types of geometry at some wall regions and turntable edges, indicating the capture of minor geometric details. The detailed comparison of the number of elements in different oven geometry types will be discussed in the result section 3.1. The average quality values of meshes are 0.66, 0.66, and 0.65, for the simple box, manually measured, and 3-D scanned geometries, respectively, which are similar to other reported value (0.64) for sufficient modeling microwave heating processes(Fia and Amorim 2021).

2.4.1.6 Simulation strategy

To comprehensively evaluate the effect of oven geometrical details on modeling accuracy, multiple frequencies and ports were used in the study. The most common frequency used for the microwave heating in domestic microwave ovens is 2.45 GHz, and the port is mostly located on the right side of the cavity. Therefore, the microwave heating processes using three oven cavity geometries were simulated at 2.45 GHz using the right port (Port #1), similar to domestic microwave ovens. The multi-port solid-state microwave system provides the flexibility to control the microwave frequency between 2.40 – 2.50 GHz, and at frequencies greater than 2.48 GHz, there are high reflections in the cavity which leads to the shutdown of the system. Therefore, to validate our model at various other frequencies and test the robustness of the developed model, additional microwave frequencies (2.40 and 2.48 GHz using Port #1) and additional ports (2.45 GHz using Port #3 and 4) were evaluated. The mashed potato was placed at the center of the turntable and heated from 4 °C for 60 s without rotation. The stationary turntable can eliminate the effect of rotation on the heating patterns, and the short heating time can minimize the effect of temperature-dependent dielectric properties and heat transfer on heating patterns.

The microwave heating simulations were carried out on a microway workstation equipped with two 16-core Intel(R) Xeon(R) 3.20 GHz wavenumber and running on a RAM of 128 GB with a Windows 10 operating system.

2.4.2 Experimental Validation

The mashed potato was used as a model food in the experimental validation because of its homogeneity and ease of preparation. The mashed potato was composed of 23.8% mashed potato flakes (Real Premium mashed potato, Idahoan Foods, Idaho Falls, ID, USA), 18.6% whole milk (Grade A homogenized whole milk, Kroger CO., Cincinnati, OH, USA), 4.1% unsalted butter

(Land O' Lakes® Unsalted Butter Sticks, Land O' Lakes, Inc, Arden Hills, MN, USA), and 53.5% deionized water. The preparation followed the procedures reported in (Chen et al. 2013). Prepared mashed potato (850 g) was filled in a plastic tray having the dimensions L×W×H of 16.5 cm × 11.7 cm × 5 cm and placed at the center of the oven cavity. In each tray, a mesh cloth made of nylon with a coarse mesh was placed at the center of the mashed potato to separate the sample into two layers, top and middle, respectively. The samples were kept in the refrigerator at 4 °C overnight for further use.

The mashed potato was heated in the fabricated solid-state microwave system. The microwave frequency, port number, and heating time were selected and matched with the simulation conditions. After the heating procedure, the food samples were rapidly removed from the microwave oven.

The thermal imaging process for the heated mashed potato involved using a thermal imaging camera (FLIR A300, Boston, MA) with a resolution of 320 × 240 pixels and accuracy of ±2°C to capture images of the top and middle layers. The camera was placed approximately 50 cm above the food product and connected to a computer. After microwave heating experiments, the food samples were removed from the oven immediately to the predetermined location under the thermal imaging camera for capturing the thermal images of the top surface. Then, the top layer mashed potato sample was removed with the pre-placed mesh cloth for capturing the thermal images at the middle layer. The whole process was completed within ~15 seconds. The captured thermal image profiles were processed in the FLIR ResearchIR software with an emissivity of 0.95, which is commonly used for food samples.

2.4.3 Quantitative comparison of temperature distribution between simulated and experimental thermal images

Previously reported microwave model validation using thermal imaging profiles often only qualitatively compared heating patterns (hot and cold spot locations) between experiments and simulation. In this study, a quantitative comparison approach was developed and used to validate the model accuracy for the thermal profiles in an irregular shape, as shown in Figure 2.6. Firstly, the experimental spatial temperature profiles captured by the thermal imaging camera were manually cropped as a rectangular region to remove the background. The cropped thermal image profiles were resized to a 320 × 240-pixeled image using the Pillow library in Python. Note that the cropped experimental images still have thermal imaging background temperatures at the corners due to the irregular shape of the food product. Then, the simulated temperature profiles were exported from COMSOL software as a regular grid of 320 × 240 pixels. Since the food surface is in an irregular shape with curvatures at corners, the cornered regions (non-food regions) did not have temperature values and were shown as NaN (Not a Number) in the matrix of 320 × 240 temperature values. Finally, a data quantification algorithm was built in Python Programming language which used NumPy and Pandas module to calculate the root mean square error (RMSE) between the corresponding pixels of the experimental temperature profiles and the simulated temperature profiles by extruding the pixels with NaN values from the simulated results using the following equation.

$$RMSE = \sqrt{\frac{1}{n}\sum_{i=1}^{n}(T_{exp} - T_{sim})^2} \quad (6)$$

where n = total number of temperature values (320 × 240 excluding NaN values), T_{exp} is the temperature of a single pixel in the experimental thermal profile, and T_{sim} is the pixeled

temperature values from the simulated thermal profile. Effectively managing the background values, the algorithm ensures a reliable and precise analysis, leading to meaningful and valid conclusions from the experimental and simulation data.

2.4.4 Data Analysis

The microwave heating experiments were performed in three replicates. One-way analysis of variance (ANOVA) was used for the statistical analysis, followed by a 95% confidence interval HSD Tukey's post-test. JMP Pro 16 (JMP, Version 16. SAS Institute Inc., Cary, NC) statistical software was used for all the calculations. Statistically significant values were those with p-values less than 0.05.

2.5 Results and Discussions

2.5.1 Comparison of meshing results among models with different geometric details

With the same meshing strategy for models having different geometric details, different meshing results were shown in Figure 2.5 (2.1.5 section), where finer mesh was observed in the 3-D scanned oven and turntable geometries. The numbers of elements in the food, turntable, air domains, and whole geometry were different for geometries with different details, as summarized in Table 2.2. Note that the total number of elements for the entire geometry was more than the sum of the three domains due to additional elements on boundaries. The number of mesh elements increased with more geometrical details in the models. First, the numbers of total elements in the food domain of the three geometries were similar and approximately equal to ~ 470,000 since the same manually drawn food geometries were used in the three models. The numbers of elements in the turntable and air domain of the manually measured geometries were slightly more than those of the simple

box geometry because the manually measured geometry can capture the major geometric details. For example, when comparing the number of elements in 3-D scanned geometry to manually measured geometry, the former had approximately 2.7 times more elements in the turntable domain and about 2.27 times more elements in the air domain. Similarly, when comparing the number of elements in 3-D geometry to the simple box geometry, the former had about 3.95 times more elements in the turntable domain and 2.85 times more elements in the air domain. These results indicate that the mesh size increases when incorporating intricate geometric details. Due to the captured minor geometric details, the number of elements in the turntable and air domains of the 3-D scanned geometry were much more than those of the other two geometries. These minor geometric details were small in size, leading to very finer mesh and a large number of elements. The much finer mesh in the 3-D scanned geometry will influence the simulation results considerably. Note that the increased number of elements also increased the computational time. For the simple box geometry, the computational time was around 6 minutes, whereas for the manually measured geometry and 3-D scanned geometry, the total computational time was approximately about 7 minutes and 12 minutes, respectively, for simulating the electromagnetic field and the one-minute heat transfer process.

2.5.2 Comparison of modeling accuracy at 2.45 GHz using the right-side port

The simulated spatial thermal profiles using three oven cavity details and three replications of experimental temperature profiles at the top and middle layers are shown in Figure 2.7. Three replications of the microwave heating experiments showed similar hot and cold spot locations with good consistency. The microwave heating experiments showed that, at the top surface, the hot spots were mainly observed at the corners and edges, besides one hot spot region at the

middle-right region of the top surface of the heated mashed potato. At the middle layer, hot spots were only observed at the corners and edges of the food.

The microwave heating models with different geometric details showed considerable differences in the predicted heating patterns. The model with simple box geometry showed good predictions of the top layer surface's hot spots at corners and edges while missing the hot spots region at the middle-right region. The models with manually measured geometry and 3-D scanned geometries showed similar simulated heating patterns that matched well with the experimental results. However, the model using manually measured geometry showed lower temperature prediction than the experimental and 3-D scanned modeling results. At the middle layer, the models using simple box geometry and manually measured geometry failed to predict the hot spots on the left side of the food product, while the model 3-D scanned geometry showed good agreement with the experimental results. This was because the oven cavity details in the model helped predict the microwave reflections on the cavity walls and, thus, the better prediction of microwave-food interactions. The predicted spatial temperature profiles from the model using the 3-D scanned geometry did not exactly match the experimental results, which might be due to missing experimental details, such as unsmooth mashed potato samples or experimental errors in thermal image capturing.

The simulated and experimental results were compared using the developed quantitative validation approach. The RMSE values of the spatial temperature distribution between spatial thermal profiles at the top and middle layers were shown in Figure 2.8. For both the top and middle layers, the RMSE values decreased with the model geometric detail, indicating significant/considerable improved model prediction accuracy by including more geometric details in the model. The quantitative comparison between experimental and simulated thermal

profiles can objectively validate the predicted heating patterns of microwave heating models instead of using subjective descriptions (e.g., generally match).

2.5.3 Comprehensive evaluation of modeling accuracy at multiple frequencies and multiple port locations

Microwave heating patterns are influenced by the microwave frequency and port locations significantly. In addition to evaluating the effect of oven geometric details on the prediction accuracy at 2.45 GHz using the right-side port (Port #1), the microwave heating models and experiments were performed at two additional frequencies (2.40 and 2.48 GHz) and port locations (Port #3 at the back and Port #4 at the left side) and quantitatively compared. The RMSE values between experimental and simulated spatial thermal profiles at multiple frequencies and port locations were summarized in Tables 2.3 and 2.4, respectively. Similar to the results for 2.45 GHz & Port #1, the models with more geometric details of the oven cavity showed improved modeling accuracy. The models using 3-D scanned geometry showed significantly or considerably decreased RMSE values **(**2.67 to 4.11 °C) when compared to the other models using the simple box **(**3.73 to 6.33 °C**)** and manually measured **(**3.20 to 4.66 °C**)** geometries at the top layer. The 3-D scanned geometry showed considerable improvement in the RMSE values at the middle layer for most scenarios, but the improvement was not significant. This may be because the temperature change at the middle layer was little since less microwave energy was converted to thermal energy due to the penetration of electromagnetic energy. Although the models using 3-D scanned geometry did not make the predicted heating patterns match with the experimental results exactly with RMSE values, close to 0 °C, the significant or considerable improvement showed the importance of including the scanned geometry details.

Therefore, 3-D scanning is promising in capturing the geometric details of microwave oven cavities to improve the model accuracy.

2.6 Conclusion

Multiphysics models to simulate the microwave heating process were developed in the COMSOL Multiphysics software to study the effect of geometric details on the modeling accuracy of the solid-state microwave heating process. The major and minor protrusions are crucial for accurately predicting the hot and cold spot locations in the food product. A more precise geometry of the oven cavity and a turntable can be obtained by a 3-D scanning approach to capture the irregular geometry of the oven cavity. Simulations were performed for three different geometries and the temperature distributions of the simulations were compared with the experimental results by a quantitative comparison approach that calculated the RMSE values between the corresponding pixels of the experimental and simulated temperature profiles. The 3-D scanned geometry improved the modeling accuracy significantly or considerably, as compared to the simple box geometry and manually measured geometry for most scenarios of multiple frequencies and port locations, although the modeling time may be extended due to the increased mesh. The 3-D scanned technology is convenient to help modelers capture irregular geometries for improved modeling accuracy. The quantitative approach in comparing spatial temperature distributions between simulation and experiments is robust to validate the models objectively.

References

Alfaifi, B., Tang, J., Jiao, Y., Wang, S., Rasco, B., Jiao, S., Sablani, S., 2014. Radio frequency disinfestation treatments for dried fruit: Model development and validation. J Food Eng 120, 268–276. https://doi.org/10.1016/j.jfoodeng.2013.07.015

Chen, F., Warning, A.D., Datta, A.K., Chen, X., 2016. Thawing in a microwave cavity: Comprehensive understanding of inverter and cycled heating. J Food Eng 180, 87–100. https://doi.org/10.1016/j.jfoodeng.2016.02.007

Chen, J., Pitchai, K., Birla, S., Gonzalez, R., Jones, D., Subbiah, J., 2013. Temperature-dependent dielectric and thermal properties of whey protein gel and mashed potato. Trans ASABE 56, 1457–1467. https://doi.org/10.13031/trans.56.10314

Chen, J., Pitchai, K., Birla, S., Jones, D., Negahban, M., Subbiah, J., 2016. Modeling heat and mass transport during microwave heating of frozen food rotating on a turntable. Food Bioprod Process 99, 116–127. https://doi.org/10.1016/j.fbp.2016.04.009

Chen, J., Pitchai, K., Birla, S., Negahban, M., Jones, D., Subbiah, J., 2014. Heat and mass transport during microwave heating of mashed potato in domestic oven-model development, validation, and sensitivity analysis. J Food Sci 79, E1991–E2004. https://doi.org/10.1111/1750-3841.12636

Fia, A.Z., Amorim, J., 2021. Heating of biomass in microwave household oven - A numerical study. Energy 218. https://doi.org/10.1016/j.energy.2020.119472

Geedipalli, S.S.R., Rakesh, V., Datta, A.K., 2007. Modeling the heating uniformity contributed by a rotating turntable in microwave ovens. J Food Eng 82, 359–368. https://doi.org/10.1016/j.jfoodeng.2007.02.050

Gulati, T., Zhu, H., Datta, A.K., 2016. Coupled electromagnetics, multiphase transport and large deformation model for microwave drying. Chem Eng Sci 156, 206–228. https://doi.org/10.1016/j.ces.2016.09.004

He, J., Yang, Y., Zhu, H., Li, K., Yao, W., Huang, K., 2020. Microwave heating based on two rotary waveguides to improve efficiency and uniformity by gradient descent method. Appl Therm Eng 178. https://doi.org/10.1016/j.applthermaleng.2020.115594

Huang, Z., Marra, F., Subbiah, J., Wang, S., 2018. Computer simulation for improving radio frequency (RF) heating uniformity of food products: A review. Crit Rev Food Sci Nutr. https://doi.org/10.1080/10408398.2016.1253000

Jiao, Y., Tang, J., Wang, S., 2014. A new strategy to improve heating uniformity of low moisture foods in radio frequency treatment for pathogen control. J Food Eng 141, 128–138. https://doi.org/10.1016/j.jfoodeng.2014.05.022

Kim, J., Moreira, R.G., Huang, Y., Castell-Perez, M.E., 2007. 3-D dose distributions for optimum radiation treatment planning of complex foods. J Food Eng 79, 312–321. https://doi.org/10.1016/j.jfoodeng.2006.01.061

Kuffi, K.D., Defraeye, T., Nicolai, B.M., De Smet, S., Geeraerd, A., Verboven, P., 2016. CFD modeling of industrial cooling of large beef carcasses. Int J Refrig 69, 324–339. https://doi.org/10.1016/j.ijrefrig.2016.06.013

Perry, M., Lentz, R., 2021. Susceptors in microwave packaging, in: Lorence, M.W., Pesheck, P.S. (Eds.), Development of Packaging and Products for Use in Microwave Ovens. Woodhead Publishing Limited, Cambridge, pp. 207–235.

Pitchai, K., Birla, S.L., Subbiah, J., Jones, D., Thippareddi, H., 2012. Coupled electromagnetic and heat transfer model for microwave heating in domestic ovens. J Food Eng 112, 100–111. https://doi.org/10.1016/j.jfoodeng.2012.03.013

Su, T., Zhang, W., Zhang, Z., Wang, X., Zhang, S., 2022. Energy utilization and heating uniformity of multiple specimens heated in a domestic microwave oven. Food Bioprod Process 132, 35–51. https://doi.org/10.1016/j.fbp.2021.12.008

Uyar, R., Erdoğdu, F., 2009. Potential use of 3-dimensional scanners for food process modeling. J Food Eng 93, 337–343. https://doi.org/10.1016/j.jfoodeng.2009.01.034

Wang, S., Yue, J., Tang, J., Chen, B., 2005. Mathematical modelling of heating uniformity for in-shell walnuts subjected to radio frequency treatments with intermittent stirrings. Postharvest Biol Technol 35, 97–107. https://doi.org/10.1016/j.postharvbio.2004.05.024

Yang, R., Chen, J., 2021. Mechanistic and machine learning modeling of microwave heating process in domestic ovens: A review. Foods 10. https://doi.org/10.3390/foods10092029

Yang R, Fathy AE, Morgan MT, Chen J. 2022. Development of online closed-loop frequency shifting strategies to improve heating performance of foods in a solid-state microwave system. Food Res Int. 154. https://doi.org/10.1016/j.foodres.2022.110985

Zhang, R., Li, F., Tang, J., Koral, T., Jiao, Y., 2020. Improved accuracy of radio frequency (RF) heating simulations using 3D scanning techniques for irregular-shape food. LWT- Food Sci Technol 121. https://doi.org/10.1016/j.lwt.2019.108951

Zhou, X., Tang, Z., Pedrow, P.D., Sablani, S.S., Tang, J., 2023. Microwave heating based on solid-state generators: New insights into heating pattern, uniformity, and energy absorption in foods. J Food Eng 357. https://doi.org/10.1016/j.jfoodeng.2023.111650

APPENDIX

Table 2.1 Physics, dielectric, and thermal properties used in the Multiphysics model.

Parameter	Values	Units	Sources
Density			
Mashed Potato	1062.5	kg/m3	Calculated experimentally
Glass	2210.0	kg/m3	COMSOL Material Library
Thermal conductivity			
Mashed Potato	0.58	W/mK	(Chen et al. 2014)
Glass	1.40	W/mK	COMSOL Material Library
Specific Heat Capacity			
Mashed Potato	4720	J/kgK	(Chen et al. 2014)
Glass	730	J/kgK	COMSOL Material Library
Dielectric Properties			
Mashed Potato			
2.40 GHz	46.99 – j × 17.99		(Yang et al. 2022)
2.45 GHz	46.89 – j × 17.94		
2.48 GHz	46.75 – j × 17.93		
Air	1.00 – j × 0		COMSOL Material Library
Glass	4.20 – j × 0		COMSOL Material Library

Table 2.2 The number of meshing elements of the models with different oven cavity geometric details

Domain	Simple box geometry	Manually measured geometry	3-D scanned geometry
Food	477,866	477,164	490,340
Turntable	101,974	148,875	403,466
Coaxial Port	77,351	38,695	38,450
Air	518,861	651,417	1,481,253
Total	1,176,052	1,316,151	2,413,509

Table 2.3 The RMSE values of simulated and experimental spatial temperature profiles at additional microwave frequencies using different geometric details with the right side port (Port #1)*.

Frequency, GHz		Simple box geometry, °C	Manually measured geometry, °C	3-D scanned geometry, °C
2.40	Top Layer	5.00 ± 0.26^{A}	4.66 ± 0.12^{A}	4.11 ± 0.13^{B}
	Middle Layer	2.51 ± 0.04^{a}	2.47 ± 0.08^{a}	2.53 ± 0.05^{a}
2.48	Top Layer	4.24 ± 0.09^{A}	3.42 ± 0.07^{B}	2.67 ± 0.30^{C}
	Middle Layer	1.73 ± 0.17^{a}	1.48 ± 0.19^{a}	1.57 ± 0.15^{a}

*Different letters in the same row indicate a significant difference ($p<0.05$).

Table 2.4 The RMSE value of simulated and experimental spatial temperature profiles using different geometric details at additional microwave port locations using 2.45 GHz*.

Port number		Simple box geometry, °C	Manually measured geometry, °C	3-D scanned geometry, °C
3	Top Layer	3.73 ± 0.08^{A}	3.20 ± 0.15^{B}	2.90 ± 0.12^{C}
	Middle Layer	2.52 ± 0.17^{a}	2.60 ± 0.20^{a}	2.15 ± 0.23^{a}
4	Top Layer	6.33 ± 0.05^{A}	3.36 ± 0.10^{B}	2.76 ± 0.06^{C}
	Middle Layer	3.00 ± 0.25^{a}	2.84 ± 0.25^{a}	2.11 ± 0.27^{b}

*Different letters in the same row indicate a significant difference ($p<0.05$)

(A)

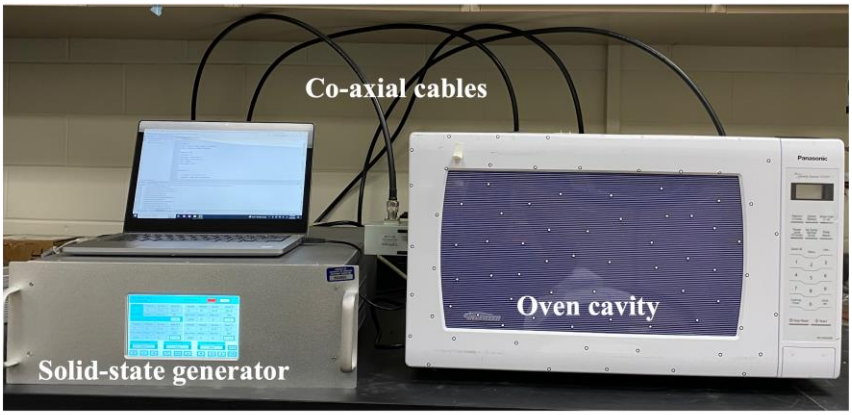

(B)

Figure 2.1 (A) A multiple-port solid-state microwave system and (B) the location of four ports inside the oven cavity.

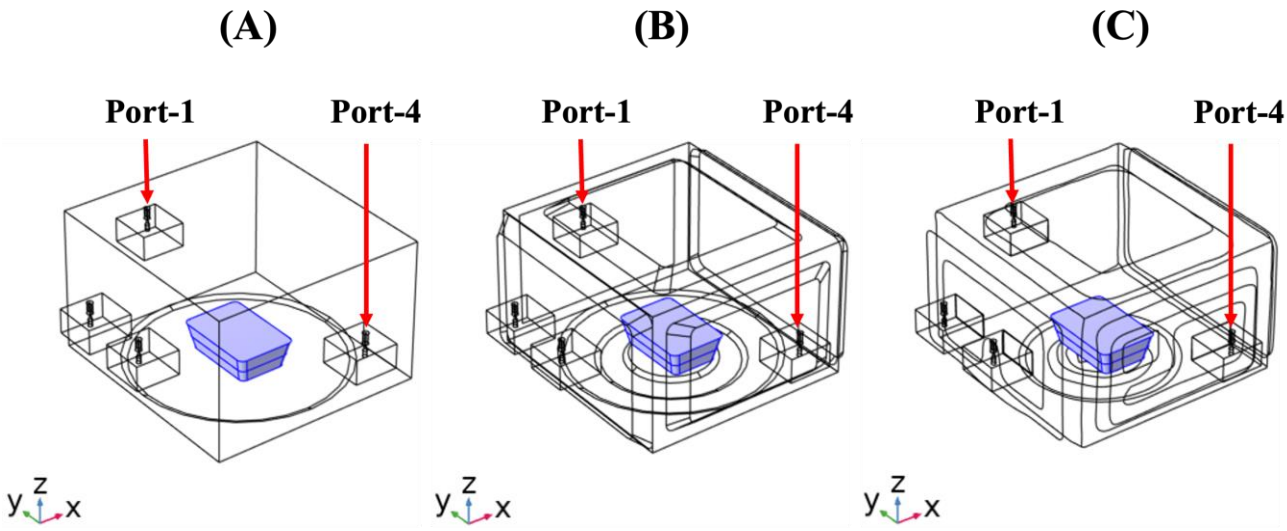

Figure 2.2 Three microwave oven geometries with different cavity details: (A) simple box, (B) manually measured, and (C) 3-D scanned.

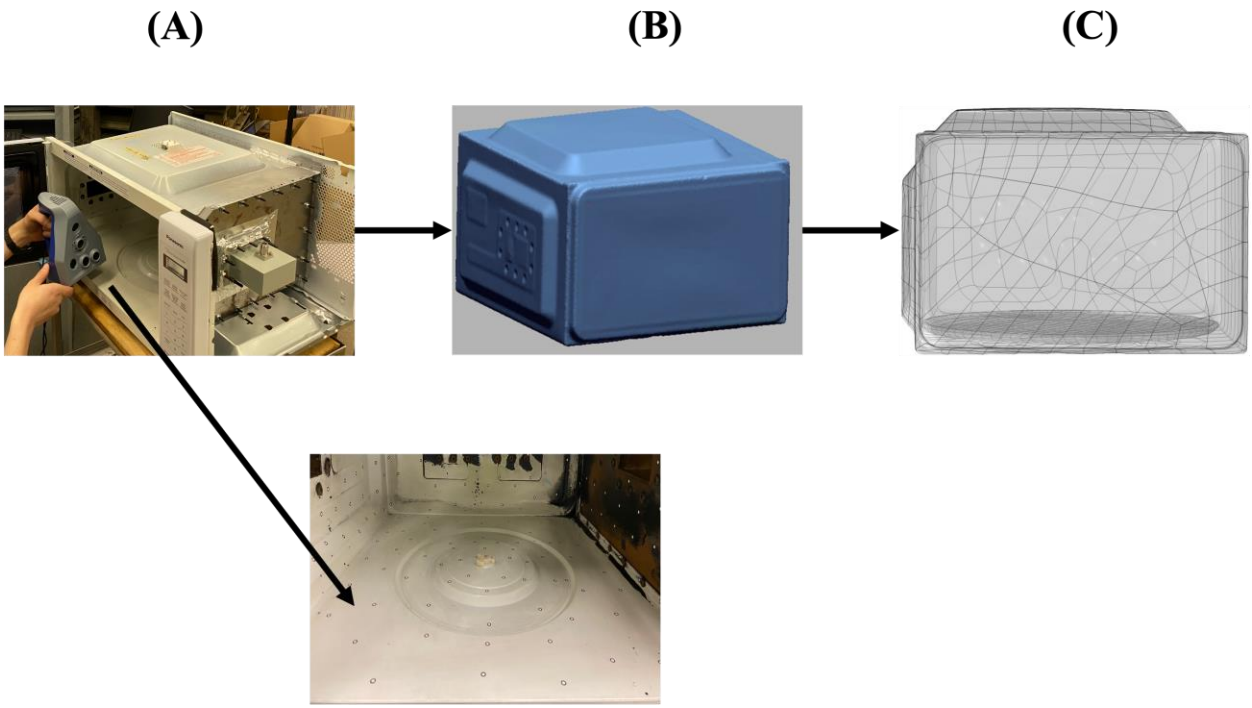

Figure 2.3 3-D scanning process of (A) scanning, (B) meshing, and (C) generating solid geometry to capture the detailed geometry of the cavity.

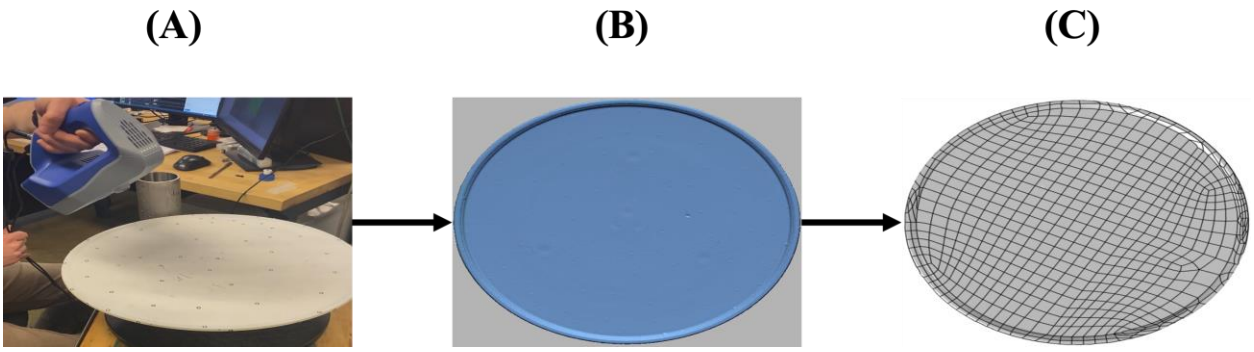

Figure 2.4 3-D scanning process of (A) scanning, (B) meshing, and (C) generating solid geometry to capture the detailed geometry of the turntable.

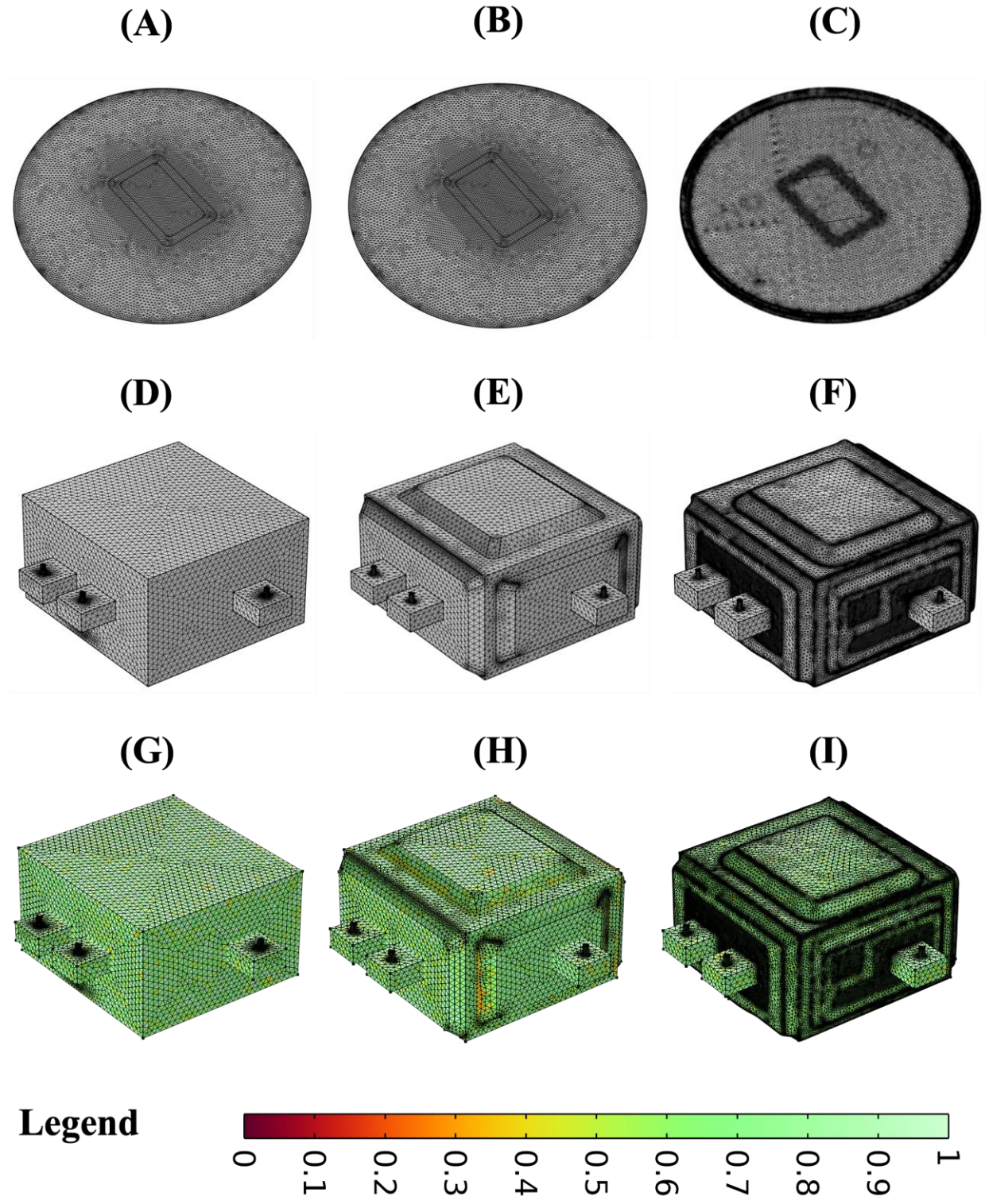

Figure 2.5 Modeling geometries and their corresponding mesh with three types of details: simple box (A & D), manually measured (B & E), and 3-D scanned (C & F) for turntable (A, B, & C) and oven (D, E, & F) and the mesh quality of the three different geometries (G, H, & I)

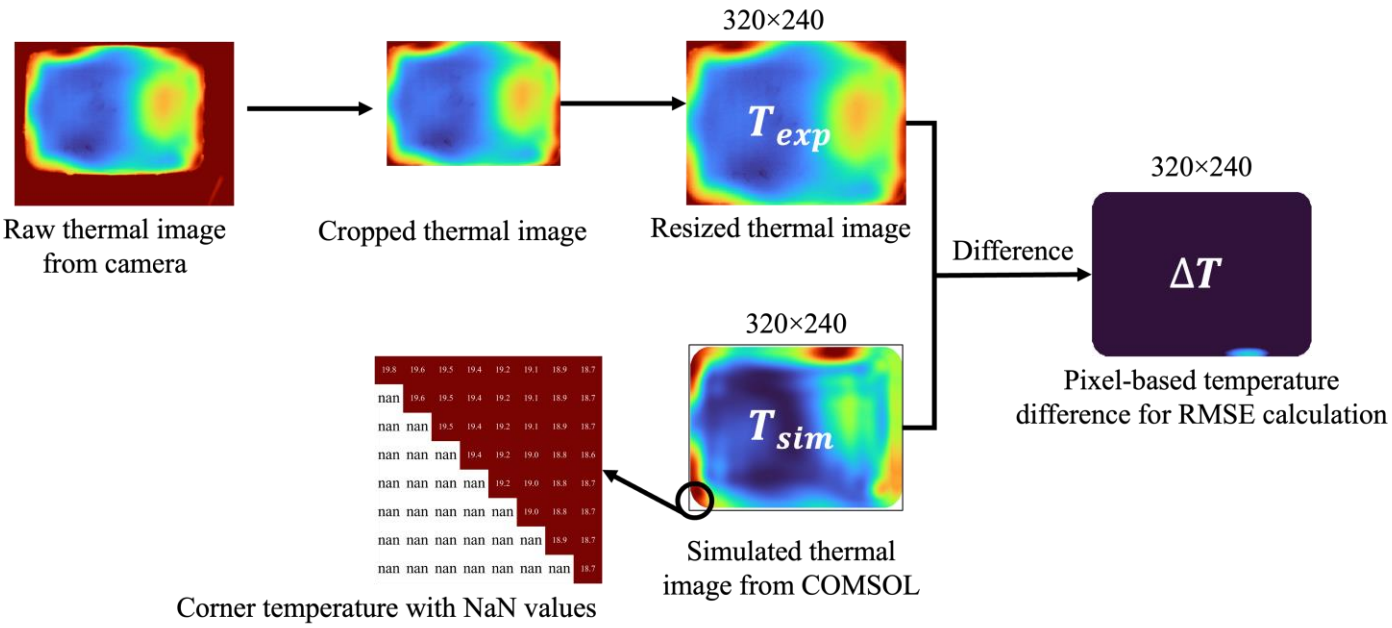

Figure 2.6 Schematic diagram showing the quantitative approach to validating spatial temperature profiles.

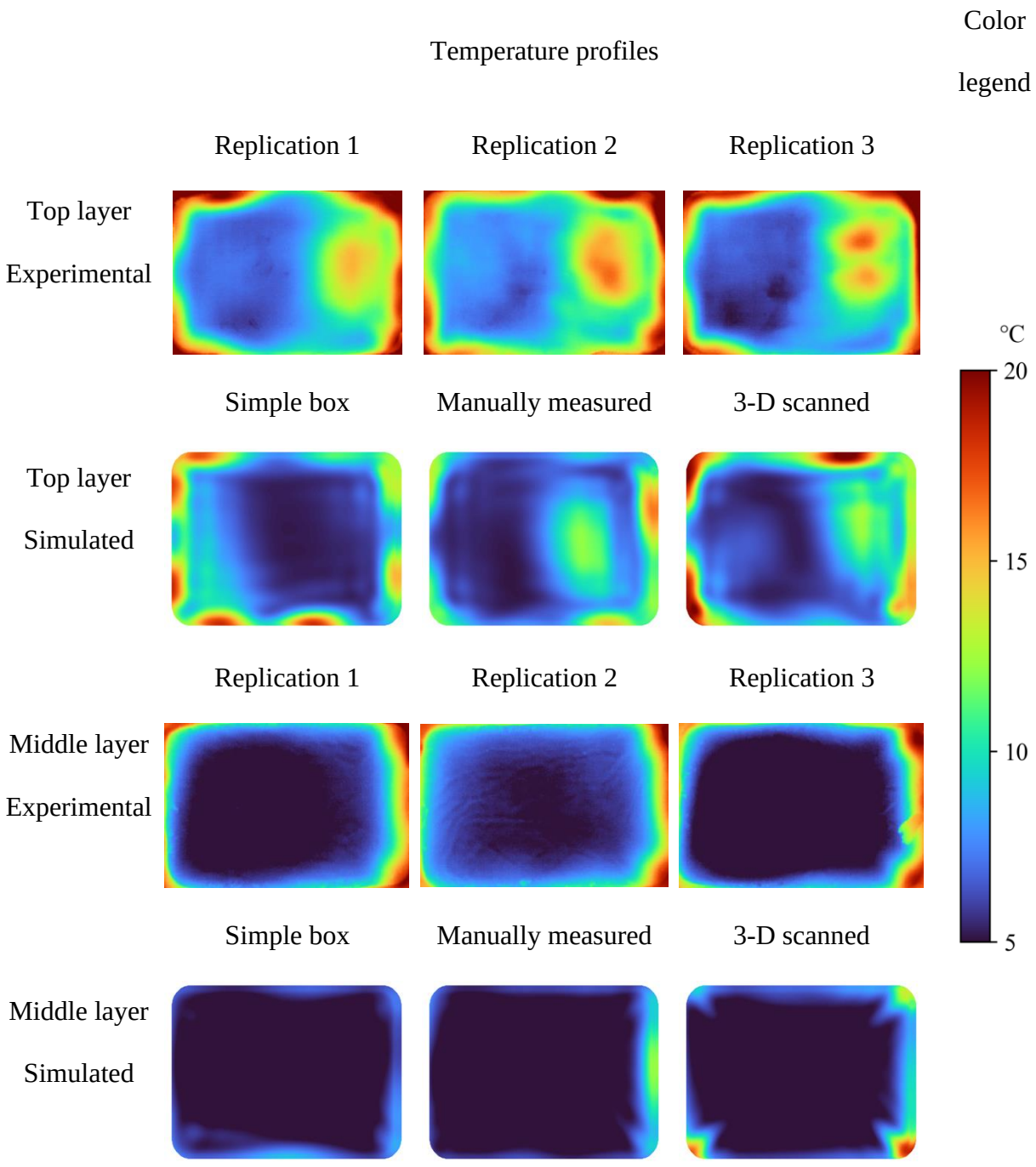

Figure 2.7 Comparison of the simulated temperature profiles of different geometries with the experimental temperature profiles for the top layer and middle layer of mashed potato.

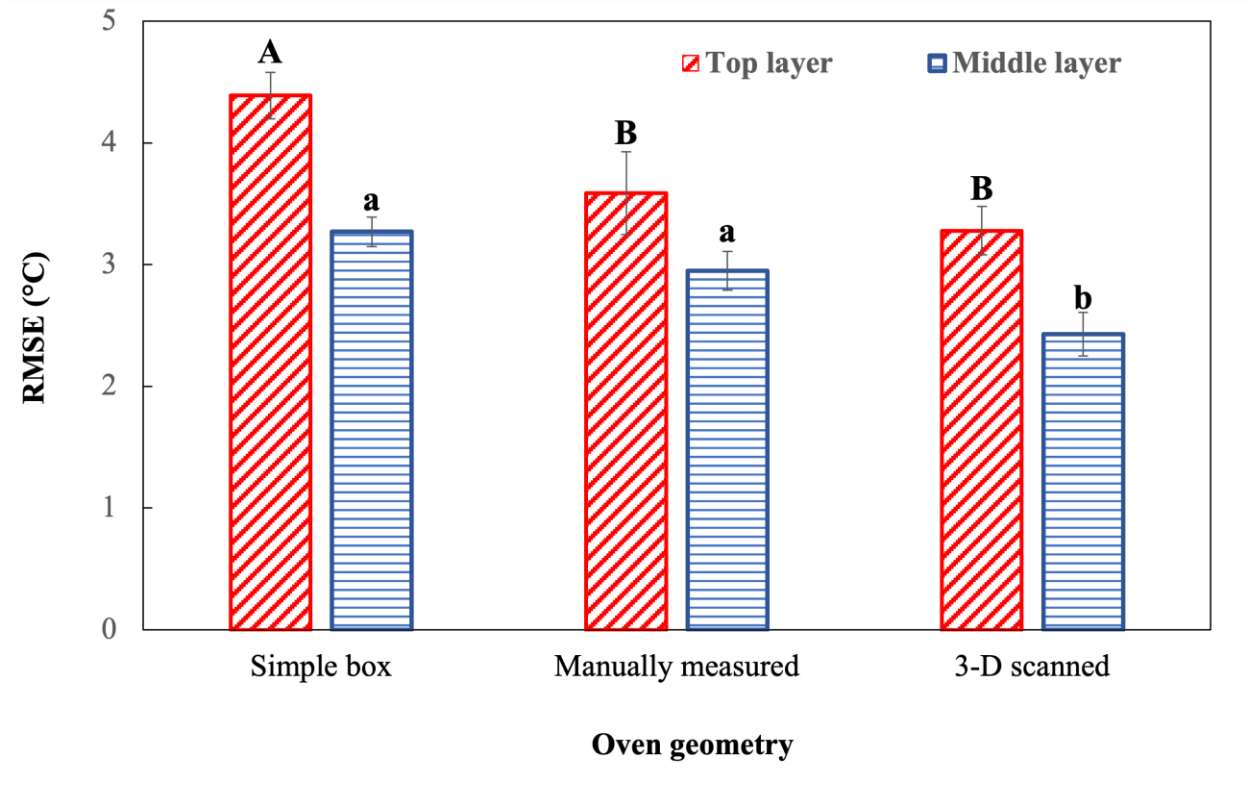

Figure 2.8 Comparison of the RMSE values* between the simulated temperature profiles of the different geometries with the experimental temperature profiles for the top and middle layer at 2.45 GHz using port 1.

*Different capital or lower-case letters indicate significant difference ($p<0.05$) at the top and middle layers.

CHAPTER III: A SIMPLE AND ACCURATE ANALYTICAL MODEL TO UNDERSTAND THE EFFECT OF RELATIVE PHASE IN A DUAL-PORT SOLID-STATE MICROWAVE HEATING PROCESS.

A version of this chapter has been submitted to the Journal of Food Engineering and is currently under review.

Verma, K., Gan H., Fathy, H., Morgan M., & Chen, J. (2023). A simple and accurate analytical model to understand the effect of relative phase in a dual-port solid-state microwave heating process. Journal of Food Engineering.

3.1 Abstract

The utilization of multi-port solid-state microwave heating systems presents a promising opportunity for improving heating performance. However, a deeper analysis of the impact of differential phase between multiple sources on microwave interactions is required. To address this challenge, the current study developed a simple analytical approach that extends the existing knowledge of plane wave interactions to encompass multi-mode standing wave interactions. By employing only four physics-based models, this analytical approach enables the prediction of microwave power densities at any arbitrary source phase difference ranging from 0° to 360°. To validate the performance of the developed analytical model, comparisons were made with results obtained from the physics-based models in terms of electric field and power densities. Upon successful validation, extensive predictions and characterizations of differential phase-dependent microwave power densities were conducted using the analytical model. The analysis of these predictions revealed wave-like patterns in the average, standard deviation, and coefficient of variations of the nodal power densities. This observation emphasizes the importance of selecting an appropriate differential phase to ensure uniform heating performance.

3.2 Keywords

relative phase, microwave interactions, standing wave, multi-mode cavity, microwave power dissipation, constructive and destructive.

3.3 Introduction

Solid-state microwave processing is an emerging technology that offers numerous advantages over traditional magnetron-based systems, including precise control of frequency, power, and relative phase (Atuonwu and Tassou 2018; Taghian Dinani et al. 2020). This technology has shown promise in improving the heating performance of food products. Previous studies have explored the effect of frequency and power on microwave heating (Tang et al. 2018; Du et al. 2019; Taghian Dinani et al. 2021; Yang et al. 2022b) and thawing (Yang and Chen, 2022), demonstrating more uniform heating patterns compared to magnetron-based ovens. Additionally, researchers have investigated the use of multiple microwave sources which can be independently controlled with precise relative phases to achieve selective and uniform heating of food products (Przemyslaw Korpas et al., 2014b; Więckowski et al., 2014). Limited studies have examined the effect of relative phases on heating performance. Wang et al. (2021) evaluated microwave heating performance using a 915 MHz dual-port microwave system and found that different heating patterns were observed at different relative phases. Ahn et al. (2023) evaluated microwave heating performance using shifted relative phases (0°, 90°, 180°, and 270°) in a GaN-based 2450 MHz microwave heating system. The results showed that, when compared to the magnetron-based microwave oven, the shifted relative phase could improve the heating uniformity by about 70.7% if the same microwave power was delivered or improve the energy

efficiency by about 31.3% if similar heating uniformity was achieved by adjusting the microwave power.

Since microwave-food interactions in multiple source system is complicated, physics-based models have been developed to verify the experimental results in these studies (Wang et al. 2021; Ahn et al. 2023; Robinson et al. 2023). However, current modeling work lacks an in-depth analysis of multi-port interactions during relative phase changes. In fact, interactions between multiple plane microwaves have been studied extensively in microwave engineering (Bows et al., 1999; Korpas et al., 2014; Korpas et al., 201). The previous knowledge of microwave interactions from multiple sources has not been used to understand multi-port interactions in solid-state microwave heating processes.

The overall goal of this study is to expand previously well-developed knowledge of multiple plane wave interactions to support a deep understanding of multi-port interactions in a multi-mode solid-state microwave oven cavity. The study hypothesized that the plane wave interaction theory can be extended to the multi-mode cavity by properly modeling the electric field within the oven cavity using limited number of physics-based modeling results.

The objectives of this study are:

(a) to develop and verify a physics-based model for simulating the electric field and dissipated power density in a dual-port microwave heating process with relative phases.

(b) to develop and validate a simple analytical model based on microwave interaction theory and physics-based models to predict the electromagnetic power distribution at different arbitrary relative phases.

(c) to characterize the effect of relative phases on microwave power dissipation using the simple analytical model.

3.4 Materials and Methods

3.4.1 Physics-based model development and verification

A physics-based model was developed to simulate the microwave-food interactions in a multi-port solid-state microwave system. The model used in this study is a simplified version of a previously validated microwave heating model developed in the previous chapter of this thesis focusing specifically on the simulation of electric field and electromagnetic power dissipation density. Heat transfer modeling was not included in this physics-based model, as its scope is limited to predicting electromagnetic power dissipation rather than temperature.

3.4.1.1 Microwave system and model geometry

In this study, a custom-designed multi-port solid-state microwave system (Figure 3.1) was utilized. The system consisted of various components, including a solid-state microwave generator (PA-2400-2500 MHz-200 W-4, Junze Technology, China), four coaxial cables connected to four waveguides (CWR340 CentricRF) through launcher ports, and a modified commercial microwave oven cavity (Panasonic Model NN-SN936W). The original magnetron and its waveguide launcher were removed from the microwave oven cavity. Notably, this multi-port solid-state microwave system allowed for precise control of the relative phase of the multi-ports with a precision of 1°. For the microwave heating process in this study, only two ports, specifically Right Port #1 and Left Port #4, were used with different relative phase differences. Both ports were operated at a microwave frequency of 2.45 GHz. For an accurate representation of the microwave oven cavity and the glass turntable, we employed a 3-D scanned geometry based on our previous chapter, as shown in Figure 3.2.

3.4.1.2 Governing equations

The electromagnetic (EM) field distribution within the oven cavity and its associated dissipated microwave power density within the food products was analyzed to understand the multi-port interactions at relative phases. The electromagnetic field distribution within the oven cavity can be described by employing a combined Maxwell's waveform equations (J. Chen et al. 2016):

$$\nabla \times \mu_r^{-1}\left(\nabla \times \vec{E}\right) - \left(\frac{2\pi f}{c}\right)^2(\varepsilon' - j\varepsilon'')\vec{E} = 0 \quad (1)$$

where, ε'refers to the dielectric constant, $\varepsilon''$is the dielectric loss factor, μ_r is the electromagnetic permeability of the food product, f is the microwave frequency in Hz, $\vec{E}$ refers to the electric field intensity in V/m, c is the speed of light in m/s, and j is $\sqrt{-1}$.

The dissipated power density (P, W/m^3) is expressed as:

$$P = \pi\varepsilon_0\varepsilon'' f|\vec{E}|^2 \qquad (2)$$

where, ε_0 refers to free space permittivity and has a value of 8.854 × 10-12 F m^{-1}, ε'' is the dielectric loss factor.

As stated before, the heat transfer was not part of this simulation.

3.4.1.3 Boundary and initial conditions

The boundary conditions in the electromagnetics were set such that the walls were considered to be perfect electric conductors, ensuring that the tangential component of the electric field is zero. This boundary condition accurately models the lossless metallic surface of the walls.

$$n \times \vec{E} = 0 \quad (3)$$

where n is the normal vector.

3.4.1.4 Material properties

The dielectric properties of air, glass (i.e., the turntable), and mashed potato (food) were acquired from the literature and/or the COMSOL material library and used in the appropriate domains, as shown in Table 3.1.

3.4.1.5 Meshing strategy

To analyze the solid-state microwave system, a tetrahedral mesh was utilized, as depicted in (Figure 3.3). Following the guidelines of Chen et al. (2014), a mesh-independent investigation was conducted to assess the impact of mesh refinement on the normalized power absorption. Different element sizes were selected for the various domains: 15 mm for the air domain, 5 mm for the turntable domain, and 3 mm for the food domain, representing the maximum element sizes employed.

3.4.1.6 Simulation strategy

In this study, the commonly used frequency of 2.45 GHz, typical in domestic microwave ovens, was selected to investigate the multi-port interactions concerning relative phases. Specifically, the two ports located on the oven cavity's left and right-side walls were utilized, with 200 W power applied to each port. To examine the effects of relative phases on the electric field distribution and microwave power dissipation density, a tray containing 400 g of mashed having dimensions L×W×H of 16.5 cm × 11.7 cm × 5 cm, potato at a temperature of 4 °C was placed at the center of a stationary turntable. During the heating process, the turntable remained immobile without any rotation.

The simulations for the microwave heating process were performed in COMSOL Multiphysics v6.0 (COMSOL Inc., Boston, MA). The simulations of electromagnetics were conducted on a

computational system featuring two 16-core Intel(R) Xeon(R) processors operating at 3.20 GHz and equipped with 128 GB of RAM.

3.4.1.7 Model verification

To verify the model, the hot and cold spot locations of the simulated electromagnetic power dissipation distribution was compared and verified against experimental heating patterns to validate the developed model on its prediction accuracy for a dual-port microwave heating process. The spatial temperature distributions over the surface of the heated mashed potato after 1 minute of the microwave heating process were captured by a thermal imaging camera (FLIR A300, Boston, MA).

3.4.2 Development of a simple analytical model of microwave interactions inside oven cavity at relative phases

To understand the microwave-food interactions with multiple excitations from the various microwave ports and the impact of their relative phases on the selective heating of food products in microwave ovens, it is crucial to comprehend the interference phenomena arising from the interaction of waves emitted by separate sources. This section will first briefly introduce the known knowledge of interactions of two plane waves with a relative phase in Section 3.4.2.1 and then extend it to microwave interactions within the oven cavity (Section 3.4.2.2), microwave interactions with changing relative phase (Section 3.4.2.3), and finally the developed simple analytical model that can predict and characterize microwave interactions inside a dual-port microwave oven cavity in section 3.4.2.4.

3.4.2.1 Microwave interactions between two plane waves with a relative phase

Figure 3.4 shows the interactions of two plane waves with the same frequency (f) but a relative phase difference of $\emptyset_r$. The two waves can be represented as Eqns. 4 and 5:

$$E_1(t) = E_1 \sin(\omega t) \quad (4)$$

$$E_2(t) = E_2 \sin(\omega t + \emptyset_r) \quad (5)$$

where $\omega = 2\pi f$, $E_1$and E_2 are the amplitudes of the two waves, and $\emptyset_r$ is the phase difference between the two waves.

The interaction of two plane waves in the same medium at a specific point in space leads to the superposition of the two individual waves resulting in a resultant wave which is the algebraic sum of the two individual waves and can be expressed as:

$$E_R(t) = E_1(t) + E_2(t) = E_1 \sin(\omega t) + E_2 \sin(\omega t + \emptyset_r) \quad (6)$$

The resultant wave equation can be further transformed by using the trigonometric identity for the sum of two sine values represented with the Eqn. 7 and with the root mean square (rms) value of the sinusoidal functions represented by Eqn. 8.

$$\sin C + \sin D = 2 \sin \frac{C+D}{2} \cos \frac{C-D}{2} \quad (7)$$

$$E_{rms} = \sqrt{\frac{\int_0^T E(t)^2 \, dt}{T}} \quad (8)$$

where T is the period of the wave, E_{rms} is the root mean square of the wave E(t).

The square of the rms form of the resultant wave can be obtained by combining the Eqs. 6, 7, and 8 with a final result as shown in the Eqn. 9:

$$E_R^2 = E_1^2 + E_2^2 + 2E_1E_2 \cos \emptyset_r \quad (9)$$

where E_R is the amplitude of the resultant wave $E_R(t)$.

This equation has been well developed in microwave engineering (Bows et al. 1999b).

3.4.2.2 Microwave interactions inside the microwave oven cavity

The fundamental principles of interference in microwave systems are the same as the interactions of two plane waves, but additional details of the waves are needed to be considered. In a

microwave system, due to the back-and-forth reflections of traveling waves from a source, a standing wave pattern is formed within the oven cavity, including the food products (assume no rotation of food or change of dielectric properties). This standing wave pattern determines how the electric field varies at different locations with fixed amplitude at a specific location.

In the case of a multi-port solid-state microwave oven, the microwaves enter the cavity through two (or more) sources for interactions. The traveling waves from these sources will bounce back and forth (within the cavity and back to the source generators) and interact with each other. The formed standing waves can be considered as two independent standing waves from the two sources; each is a combination of waves that have three components in (x, y, and z-directions). Therefore, at any given location within the oven cavity (including food products), the combined microwave electric field contributed by the two microwave sources can be considered as the sum of six waves, as shown in Eqn. 10.

$$E_R(t) = (E_{1x}(t) + E_{2x}(t))a_x + (E_{1y}(t) + E_{2y}(t))a_y + (E_{1z}(t) + E_{2z}(t))a_z \qquad (10)$$

where the subscripts 1 and 2 indicate the individual microwave sources, and subscripts x, y, and z indicate the three different components of the electric field, and a_x, a_y, a_z are unit vectors in each direction.

Note that due to the irregular shape of the oven cavity and multimode characteristics and complicated food products, there are relative undetermined phase differences between $E_{1x}(t)$ and $E_{2x}(t)$, $E_{1y}(t)$ and $E_{2y}(t)$ and $E_{1z}(t)$ and $E_{2z}(t)$ at any specific locations within the oven cavity and the relative phase angles are different for the x, y, and z directions and different locations within the cavity and foods.

Therefore, at any given location within the oven cavity (including food products), the combined microwave electric field can be considered as the sum of six waves as shown in Eqn. 11.

$$E_R(t) = (E_{1x}\sin(\omega t) + E_{2x}\sin(\omega t + \emptyset_{rx}))a_x + (E_{1y}\sin(\omega t) + E_{2y}\sin(\omega t + \emptyset_{ry}))a_y +$$

$$(E_{1z}\sin(\omega t) + E_{2z}\sin(\omega t + \emptyset_{rz}))a_z \qquad (11)$$

where, E_{1x}, E_{1y}, and E_{1z} are the peak electric field intensities (amplitudes) of the standing wave at three directions of x, y, and z contributed by microwave source 1, E_{2x}, E_{2y}, and E_{2z} are the peak electric field intensities of the standing wave at the same location due to source 2, $\emptyset_{rx}$, $\emptyset_{ry}$, and $\emptyset_{rz}$ are the relative phase difference between $E_{1x}$and E_{2x}, E_{1y} and E_{2y}, E_{1z} and E_{2z} respectively, and are functions of x, y, and z.

The square of the root mean square (rms) of the combined wave at any single point from the interaction of these two standing waves can be written as:

$$E_R^2 = E_{1x}^2 + E_{2x}^2 + 2E_{1x}E_{2x}\cos\emptyset_{rx} + E_{1y}^2 + E_{2y}^2 + 2E_{1y}E_{2y}\cos\emptyset_{ry} + E_{1z}^2 + E_{2z}^2 +$$

$$2E_{1z}E_{2z}\cos\emptyset_{rz} \qquad (12)$$

3.4.2.3 Microwave interactions inside the microwave oven cavity with relative phase change

The concept of the source phase difference plays a crucial role in understanding the interference phenomena in wave interactions within the solid-state microwave process. The source phase difference refers to the phase disparity between the two sources responsible for creating controlled standing waves inside the oven cavity. When the relative source phase difference is changed, it directly influences the local relative phase between the two standing waves at any given point within the cavity, where Eqn.12 can be modified by adding the source phase difference ($\emptyset_s$) as Eqn. 13:

$$E_R^2 = E_{1x}^2 + E_{2x}^2 + 2E_{1x}E_{2x}\cos(\emptyset_{rx} + \emptyset_s) + E_{1y}^2 + E_{2y}^2 + 2E_{1y}E_{2y}\cos(\emptyset_{ry} + \emptyset_s) + E_{1z}^2 +$$

$$E_{2z}^2 + 2E_{1z}E_{2z}\cos(\emptyset_{rz} + \emptyset_s) \qquad (13)$$

3.4.2.4 Simple analytical model to determine microwave-food interactions in a dual-port microwave system.

The essential concept of the simple analytical model to determine microwave-food interactions is that the electric field intensity of the resultant wave at one specific location has a relationship between the electric field intensities contributed by two individual ports at x, y, z-directions, their initial local (nodal) relative phases differences between two standing waves at x, y, and z directions at zero source phase difference, and the source phase differences to be applied, as described by Eqn. 13. The electric field intensities at x, y, and z directions contributed by the two microwave sources and their initial local relative phase differences at x, y, and z directions can be obtained from four physics-based electromagnetics models, as described below in detail.

The first two models simulate the electromagnetic field distribution using two ports individually (Port 1 and Port 4), which can determine the electric field intensities (E_1 and E_2) contributed by the individual two ports at three directions (x, y, and z). It is important to note that, for the two models using individual port (Port 1 or Port 4) heating, the other port (Port 4 or Port 1) is still on but with 0 power input. The activation of two ports simultaneously (one with full power and the other with 0 power) allows port interactions that influence the EM field distribution within the cavity, although one port is zero-power input. After simulating the first two models, the third model involves simultaneous operation of Port-1 and Port-4 with a 0° relative source phase difference (any arbitrary relative source phase difference also works, but 0° can simplify the problem for understanding) and full power for both ports. The model results can determine the resultant electric field intensities at three directions (x, y, z). For each direction (x, y, or z), an initial local (nodal) relative phase difference ($\emptyset_r$) can be calculated from E_1, E_2, and E_R at corresponding three directions by a modified form of Eqn. 9 as Eqn. 14:

$$\emptyset_r = \cos^{-1}\left(\frac{E_R^2 - E_1^2 - E_2^2}{2E_1E_2}\right) \qquad (14)$$

It is important to note that for one $\cos \emptyset_r$ value calculated from E_1, E_2, and E_R, both $\emptyset_r$ (Point A) and 360-$\emptyset_r$ (Point B) meet the condition, as shown in the Figure 3.5. To determine the exact local (nodal) relative phase differences, the fourth model that simulates simultaneous dual-port heating at another source phase difference (e.g., 90°) can be used to determine cos $(\emptyset_r + 90)$ and thus $\emptyset_r$, since cos $(360 - \emptyset_r + 90)$ should have a different value. Therefore, based on four physics-based modeling results, the resultant electric field intensities at any other source relative phase difference can be predicted by Eqn. 13.

Based on the predicted electric field intensities, the power dissipation density within the food product, which relates to the conversion of electromagnetic energy to thermal energy, can be determined by Eqn. 15:

$$P = \pi \varepsilon_0 \varepsilon'' f {E_R}^2 \qquad (15)$$

where ε_0 is the permittivity of free space, ε'' is the dielectric loss factor, f is the microwave frequency in Hz, and E_R is the predicted electric field intensity in V/m at any location.

3.4.3 Validation of the analytical model for determining dissipated microwave power density

In order to validate the simple analytical model, the predicted electric field intensities in the x, y, and z directions and the microwave power dissipation density distribution at several arbitrarily selected relative source phase angles (e.g., 37°, 135°, 180°, and 223°), were compared with the results obtained from the physics-based modeling. The local microwave power dissipation densities, also known as nodal values, were extracted from both analytical and physics models, and compared for validation purposes. It is expected that the analytical and physics models are

supposed to have exact same modeling results, demonstrating the validity of the proposed analytical approach in extending the plane wave interactions to a solid-state multi-mode oven cavity. Once validated, this analytical model can be used to predict power dissipation density distribution to understand the microwave-food interactions in multisource microwave heating processes.

3.4.4 Characterization of the microwave power dissipation

The validated simple analytical model was employed to analyze the distribution of nodal microwave power dissipation density at different relative source phase differences ranging from 0° to 360°, with a step size of 10°. The results analyzed using JmP software generated a box plot representing the five-point summary (minimum, first quartile, median, third quartile, and maximum values) of the microwave power dissipation within the food product. Furthermore, the average, standard deviation, and coefficient of variation (COV) of the nodal microwave power dissipation density were calculated.

By comparing the nodal microwave power dissipation from simultaneous dual-port microwave heating processes at various source phase differences with the sum of the individual single port microwave heating processes, we aimed to understand wave interference occurring in a solid-state microwave oven comprehensively. This comparison allowed us to observe the constructive and destructive electric field interactions that take place between the two separate sources at various nodal points within the food product. Such insights are valuable for understanding the intricate dynamics of microwave wave interference in a multi-port system.

3.5 Results and Discussion

3.5.1 Experimental verification of the physics-based model

The comparison between the simulated (physics-based model) microwave power density distribution and the experimental temperature profiles at the top surface of the food products was conducted for the dual-port microwave heating process with a relative source phase difference of 0°, as depicted in Figure 3.6. The experimental temperature profiles revealed that the corners of the food products experienced higher heating levels due to the edge heating effect, indicating non-uniform dissipation of microwave power. Additionally, minor hot spots were observed in the middle region of the food products. The physics-based model successfully captured the hot spots at the corners and edges, as well as a relative hot spot region similar to that observed in the experiments. However, slight differences were observed between the simulated power density distribution and the experimental temperature profiles. These differences could be attributed to inaccuracies in the assumed dimensions of the oven cavity and the food properties utilized in the simulation, although efforts were made to characterize the parameters as accurately as possible. It is important to note that the exact validation of microwave heating results at 2.45 GHz poses a challenge due to the complex microwave-food interactions within the multimode oven cavity, which are influenced by various parameters, including oven characteristics, food properties, and packaging conditions (Geedipalli et al. 2008; Vadivambal and Jayas 2010; Perry and Lentz 2021). Wang et al. (2021) performed simulations on the effect of relative phases using a dual-port 915 MHz microwave system with a simplified oven cavity and waveguides. Their experimental results showed good agreement with the simulation results and did not exhibit edge heating. The relatively lower frequency and simpler oven design contributed to the successful matching of temperature profiles between experiments and simulations in Wang's study.

Although there are some discrepancies in this study, the overall verification of the simulated power density distribution with the temperature profiles provides encouraging results for further analysis and prediction of power density distribution at other relative phase differences.

3.5.2 Validation of simple analytical model using physics-based model results

A simple analytical model was used to predict the nodal vector electric field intensity components within the entire oven cavity, including the air, food, and turntable domains. An arbitrary source phase difference of 135° was considered for the analysis, and the predicted results were compared with the simulated results from the physics-based model, as shown in the scatter plot of Figure 3.7. Each dot in the figures represents one nodal electric field, and all the dots collectively represents the electric field distribution within the entire oven cavity.

The scatter plot indicates that the electric field intensity exhibits a wide range of values, ranging from approximately 0 to 25×10^9 V/m, suggesting a non-uniform distribution of the electric field. Additionally, considerable differences are observed along the three directions, with the electric field densities in the z direction being much smaller than those in the x and y directions. In terms of validation of the simple analytical model, the coefficient of determination (R^2) of the scatter plot of the analytical and simulated electric field was 1 for all three directions, indicating an exact match between the results of the simple analytical model and the physics-based model. The R^2 value of 1 is as expected, and it demonstrates the validity of the proposed analytical model for multiport interactions.

For further validation, the simple analytical model was also employed to predict the nodal dissipated power density within the food product domain at four arbitrary source phase differences (37°, 135°, 180°, and 223°). The results from the simple analytical model were compared with the simulated results from the physics-based models at all the nodal points, as

shown in Figure 3.8. Across all relative source phase differences, the nodal dissipated power density exhibits a wide range of values, ranging from approximately 2,000 to 10^7 W/m^3, indicating a nonuniform distribution of microwave power within the food product itself. The nodal dissipated power density also shows different maximum values, indicating variations in power distribution at different phase differences, which can significantly influence the heating performance. Similar to the validation of the electric field distribution, the coefficient of determination (R^2) for the nodal dissipated electromagnetic power density is the same (i.e., 1) for all arbitrary source phase differences, further confirming the validity of the simple prediction model.

3.5.3 Characterization of the microwave power dissipation

Following the successful development of the simple analytical model for the dual-port microwave heating process, further analysis was conducted to predict and characterize microwave power dissipation densities for a wide range of differential phase differences covering 0° to 360°. This extensive analysis aimed to gain a deeper understanding of the impact of relative phase differences on heating performance. By examining the power dissipation densities at different relative phase differences, valuable insights can be obtained regarding the optimal selection of relative phases to achieve desired heating outcomes.

3.5.3.1 Effect of relative phase differences on dissipated microwave power density distribution patterns

Figure 3.9 displays the microwave power density distribution at the top surface of the food product across various relative source phase differences from 0° to 360° with a step size of 30°. It is evident that the locations of hot spots, characterized by high microwave power densities, undergo significant changes as the relative phase differences vary. Notably, while hot spots are

predominantly found at the edges of the food product, their specific locations differ based on the relative phase differences. For instance, at a relative phase difference of 0°, multiple edges and corner locations exhibit high microwave power densities. Conversely, at a relative phase difference of 180°, only two major hot spots are observed at the upper and bottom edges. Since the dissipated microwave power density distribution determines the heating patterns in the microwave process, the diverse heating patterns observed due to variation in the relative source phase differences offer opportunities for improving the overall heating uniformity. For example, Wang et al. (2021) demonstrated a 39.1% improvement in the heating uniformity of potato by sweeping through relative phase differences from 0° to 360° with a small step size of 1.2° in a 915 MHz microwave system. The relative phase difference-dependent thermal patterns observed in this study can potentially be utilized to develop a similar strategy of adjusting the relative phase differences to enhance the microwave heating performance in the 2.45 GHz solid-state microwave system.

3.5.3.2 Effect of relative phase differences on the nodal dissipated microwave power density

Figure 3.10 shows the nodal dissipated microwave power density at four arbitrary points within the food products at edge and center locations (Figure 3.10 A). The relative phase-dependent nodal microwave power density (Figure 3.10 B&C) showed wave-like patterns for the four points but with quite different values. The wave-like pattern can be understood from Eqns. 13 and 15, where microwave power density is a cosine function of source phase difference at each specific point. Due to different initial local relative phase at these points, the cosine wave pattern did not align with each other and will present maximum power density at different relative phases. The different microwave power densities values are related to the penetration depth of the food product, where low microwave power was observed at the center locations since

microwaves cannot penetrate deep into the food product. The wave-shape nodal microwave power density at various relative phases implied that changing the source relative phase at different heating time steps will adjust the microwave power densities at a specific location that may help slightly improve the microwave heating uniformity. However, the improvement may not be significant, since microwave power density at a specific point can only change within a range along with relative phase, which is highly dependent on the penetration depth and the location of the point.

Figure 3.11 represents the box plot (minimum, first quartile, median, third quartile, and maximum values) illustrating all the nodal dissipated microwave power density within the food products at various values of relative source phase differences varying from 0° to 360° with a step size of 10°. It can be observed that, at any relative phase difference, the nodal power density showed a wide range of 0 to about 3×10^6 W/m^3, indicating nonuniform distribution of microwave power densities that may result in uneven heating performance. Considerable difference was also observed among different relative phase differences.

In general, the first quartile, median, third quartile, and maximum values of the nodal microwave power density distribution vary with the relative phase differences. These values decrease as the relative phase difference approaches the bottom value, then slightly increase to the peak value, and subsequently decrease to the baseline value at 0° (since 360° is equivalent to 0° due to a full wave cycle). The specific locations of the bottom and peak values (relative phase difference values) slightly differ between the quartiles, median, and maximum values. This periodic pattern demonstrates that microwave-food interactions undergo slight variations due to the microwave interactions originating from the two sources, resulting in constructive and destructive microwave patterns.

Figure 3.12 illustrates the average (Figure 3.12A), standard deviation (Figure 3.12A), and COV (Figure 3.12B) of the nodal power density within the food products at various relative phase differences from 0° to 360° with a step size of 10°. Similar periodic patterns are observed, wherein the average nodal power density decreases with the relative phase difference to the bottom value (around 130°), then slightly increases to the peak value (around 320°), and finally decreases to the baseline value at 0° (since 360° is equivalent to 0° due to a full cycle). The lower average microwave power density at most relative phase differences indicates lower energy efficiency, while the higher average microwave power density at specific relative phase differences is beneficial for the heating process with slightly higher energy efficiency. However, it is important to note that the standard deviations are also large for relative phase differences with high average power density, indicating a more nonuniform power and temperature distribution after heating.

The COV exhibits a similar behavior with relative phase differences, as depicted in Figure 3.12B. Initially, the COV experiences a slight increase from 1.10 at 0° to 1.19 at 170°, followed by a subsequent decrease until it reaches a value of 0.98 at 290°, and then increases again till 1.10 at 360°. It is noteworthy that the relative source phase difference value with the minimum COV differs from that of the highest average microwave power density, suggesting that the relative phase difference needs to be carefully selected to balance heating energy efficiency and uniformity if a single relative phase difference is employed.

3.5.3.3 Understanding of the effect of dual-port interaction on microwave power dissipation

The microwave interaction within the food product due to the use of two independent sources is not a simple addition of the two waves. The predicted nodal dissipated power density was analyzed by comparing the power densities of running the two ports simultaneously with the sum

of the power densities of the two ports when individually operated. Figure 3.13 shows the results at four arbitrary relative phase differences.

The analysis reveals that significant microwave interactions occur during the dual-port microwave heating process, as the simultaneous power densities vary significantly from the sum of the individual power densities at all relative phase differences. At certain nodal points, the simultaneous power densities can be as low as 0 W/m^3, indicating almost complete destructive interference of the two individual power densities. On the other hand, at some nodal points, the simultaneous power densities can be as high as twice the sum of the two individual power densities, illustrating the constructive microwave interactions that significantly increase the dissipated power density.

These findings demonstrate that the addition of the two waves does not follow a simple scalar addition involving only the magnitudes. Instead, microwave interactions follow vector addition, taking into account both the magnitude and phase of the waves. This behavior can be understood through Eqn. 13, where the cosine of the local relative phase plays a crucial role in determining whether the superimposition of the two waves results in constructive or destructive interference. The constructive and destructive microwave interactions can lead to a significantly nonuniform power distribution, with some locations having power densities twice the sum and others having null power densities. Therefore, further extensive study of microwave interactions contributed by multiple port interactions is necessary. The simple analytical model developed in this study is valuable as it enables the generation of a large amount of data at different relative phase differences using limited physics-based modeling results. This dataset can be analyzed using statistical and machine learning approaches for further study and optimization.

Characterizing power densities at various relative phase differences is particularly valuable for determining the optimal relative source phase angles for selective microwave heating and achieving uniformity. By identifying specific phase angles that result in selective microwave heating, sweep loops can be formed, involving cycling through different phase angles during the heating process. This selective microwave heating technique with specific phase angles could enhance the uniformity of the food product and improves overall food quality. Such characterizations provide valuable insights into the microwave heating process and open possibilities for optimizing heating techniques using relative phases for various food applications.

3.5.4 Significance and future work

The simple analytical model extends the general knowledge of plane wave interactions to study multiport interactions within a multimode oven cavity. The extensive validation with electric field and microwave power dissipation densities approves the validity of the developed simple analytical model. The validated model provides a more efficient solution than extensive physics-based modeling of all relative phase angles. This analytical approach could enable deep understanding of multiport interactions with relative phase.

This current analytical model can only predict electric field and microwave power densities at given dielectric properties. During real microwave heating process, the temperature-dependent dielectric properties would influence the multiport interactions, which needs an updated analytical model. However, since only four physics-based models were needed to develop the analytical model, it is much more efficient than the extensive physics-based modeling approach to study the multiport interactions with relative phase change. A large dataset that studies the effect of relative phase on microwave heating of foods with changing properties within solid-

state microwave oven cavities can be generated and utilized in machine learning approach for further understanding of the contribution of relative phase.

3.6 Conclusion

To explore the influence of relative source phase differences on microwave interactions within a multi-source solid-state microwave system, a simple analytical model was developed based on the knowledge of plane wave interactions. The model utilized four physics-based modeling results and accurately calculated the electric field and power density distributions. The analytical model demonstrated a precise match with the results obtained from physics-based modeling, demonstrating the validity of the developed simple analytical approach. Extensive characterization of the microwave power density distribution using the analytical model revealed a wide range of nodal power densities, indicating a nonuniform distribution. Moreover, the average and standard deviation of the nodal power densities varied depending on the relative source phase differences. Hence, it is necessary to properly select relative phases to ensure heating energy efficiency and uniformity. The simple analytical model provides a more efficient solution than extensive physics-based modeling of all relative phase angles and enables a deep understanding of multiport interactions with relative phase.

References

Ahn, S.H., Jeong, C.H., Lee, W.S., 2023. 0.5kWatt 2.45 GHz GaN-based microwave heating system design with active phase control. Microw Opt Technol Lett. https://doi.org/10.1002/mop.33689

Atuonwu, J.C., Tassou, S.A., 2018. Quality assurance in microwave food processing and the enabling potentials of solid-state power generators: A review. J Food Eng. https://doi.org/10.1016/j.jfoodeng.2018.04.009

Bows, J.R., Patrick, M.L., Janes, R., Ricky' Metaxas, A.C.', Dibben, D.C., 1999. Microwave phase control heating. Int J Food Sci Technol 34, 295–304.

Chen, J., Pitchai, K., Birla, S., Jones, D., Negahban, M., Subbiah, J., 2016. Modeling heat and mass transport during microwave heating of frozen food rotating on a turntable. Food Bioprod Process 99, 116–127. https://doi.org/10.1016/j.fbp.2016.04.009

Chen, J., Pitchai, K., Birla, S., Negahban, M., Jones, D., Subbiah, J., 2014. Heat and mass transport during microwave heating of mashed potato in domestic oven-model development, validation, and sensitivity analysis. J Food Sci 79, E1991–E2004. https://doi.org/10.1111/1750-3841.12636

Du, Z., Wu, Z., Gan, W., Liu, G., Zhang, X., Liu, J., Zeng, B., 2019. Multi-physics modeling and process simulation for a frequency-shifted solid-state source microwave oven. IEEE Access 7, 184726–184733. https://doi.org/10.1109/ACCESS.2019.2960317

Geedipalli, S.S.R., Rakesh, V., Datta, A.K., 2007. Modeling the heating uniformity contributed by a rotating turntable in microwave ovens. J Food Eng 82, 359–368. https://doi.org/10.1016/j.jfoodeng.2007.02.050

Korpas, Przemyslaw, Krysicki, M., Więckowski, A., 2014a. Phase-Shift-Based Efficiency Optimization in Microwave Processing of Materials with Solid-State Sources. 16th Seminar Computer Modeling in Microwave Power Engineering, Karlsruhe, Germany, 2014.

Korpas, Przemyslaw, Wieckowski, A., Krysicki, M., 2014b. Effects of applying a frequency and phase-shift efficiency optimisation algorithm to a solid-state microwave oven, in: 2014 20th International Conference on Microwaves, Radar and Wireless Communications, MIKON 2014. Institute of Electrical and Electronics Engineers Inc. https://doi.org/10.1109/MIKON.2014.6899994

Perry, M., Lentz, R., 2021. Susceptors in microwave packaging, in: Lorence, M.W., Pesheck, P.S. (Eds.), Development of Packaging and Products for Use in Microwave Ovens. Woodhead Publishing Limited, Cambridge, pp. 207–235.

Taghian Dinani, S., Feldmann, E., Kulozik, U., 2021. Effect of heating by solid-state microwave technology at fixed frequencies or by frequency sweep loops on heating profiles in model food samples. Food Bioprod Process 127, 328–337. https://doi.org/10.1016/j.fbp.2021.03.018

Taghian Dinani, S., Kubbutat, P., Kulozik, U., 2020. Assessment of heating profiles in model food systems heated by different microwave generators: Solid-state (semiconductor) versus traditional magnetron technology. Innov Food Sci Emerg Technol 63. https://doi.org/10.1016/j.ifset.2020.102376

Tang, Z., Hong, T., Liao, Y., Chen, F., Ye, J., Zhu, H., Huang, K., 2018. Frequency-selected method to improve microwave heating performance. Appl Therm Eng 131, 642–648. https://doi.org/10.1016/j.applthermaleng.2017.12.008

Wang, C., Yao, W., Zhu, H., Yang, Y., Yan, L., 2021. Uniform and highly efficient microwave heating based on dual-port phase-difference-shifting method. Int. J. RF Microw. Comput.-Aided Eng. 31. https://doi.org/10.1002/mmce.22784

Więckowski, A., Korpas, P., Krysicki, M., Dughiero, F., Bullo, M., Bressan, F., Fager, C., 2014. Efficiency Optimization For Phase Controlled Multi-Source Microwave Oven. Int. J. Appl. Electromagn 44, 235–241. https://doi.org/10.3233/JAE-141764

Yang, R., Fathy, A.E., Morgan, M.T., Chen, J., 2022. Development of a complementary-frequency strategy to improve microwave heating of gellan gel in a solid-state system. J Food Eng 314. https://doi.org/10.1016/j.jfoodeng.2021.110763

APPENDIX

Table 0.1 Dielectric properties used in the models.

Materials	Values	Sources
Mashed Potato	46.89 – j × 17.94	(Yang et al. 2022)
Air	1.00 – j × 0	COMSOL Material Library
Glass	4.20 – j × 0	COMSOL Material Library

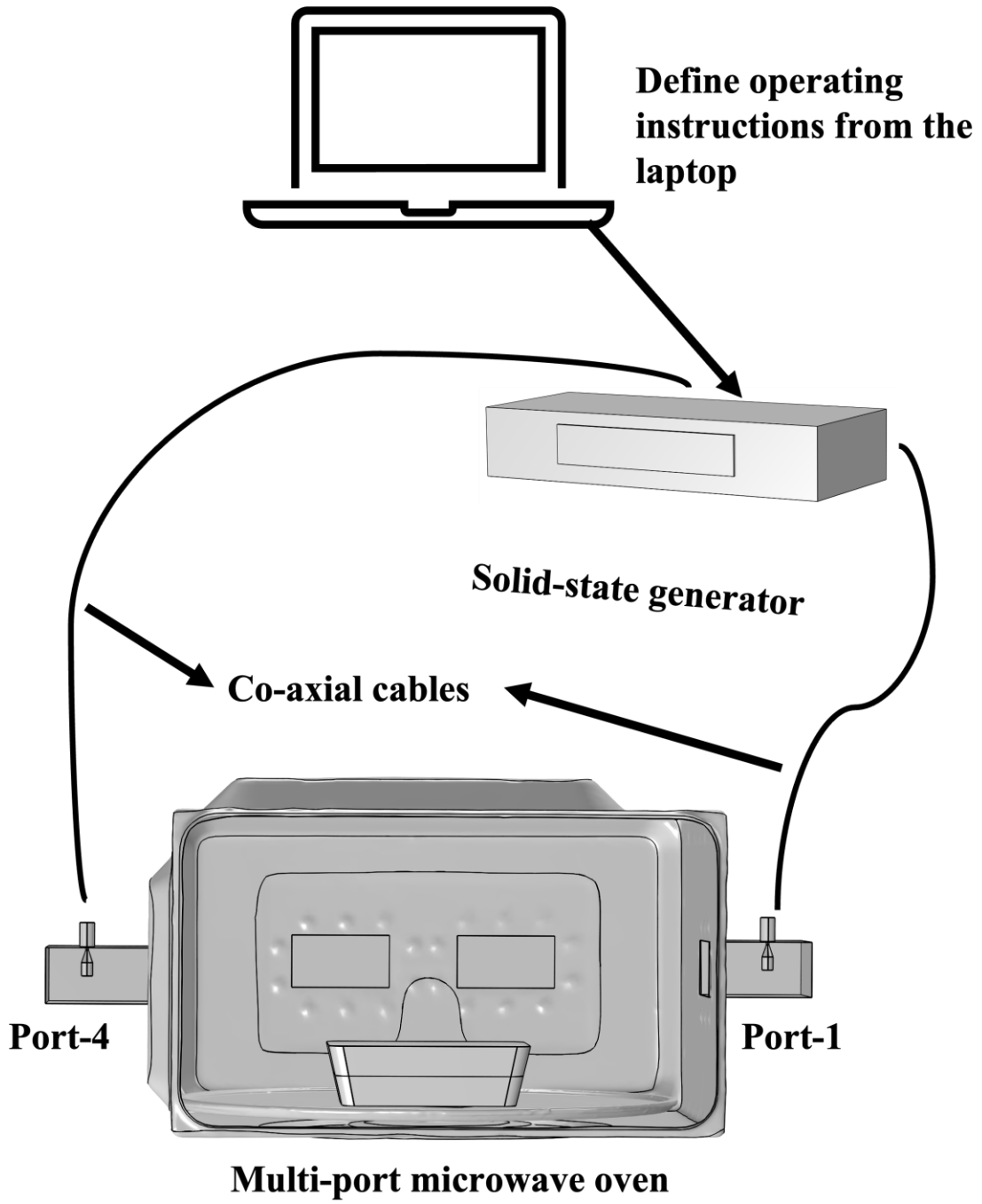

Figure 3.1 A schematic diagram of a multiple-port solid-state microwave system

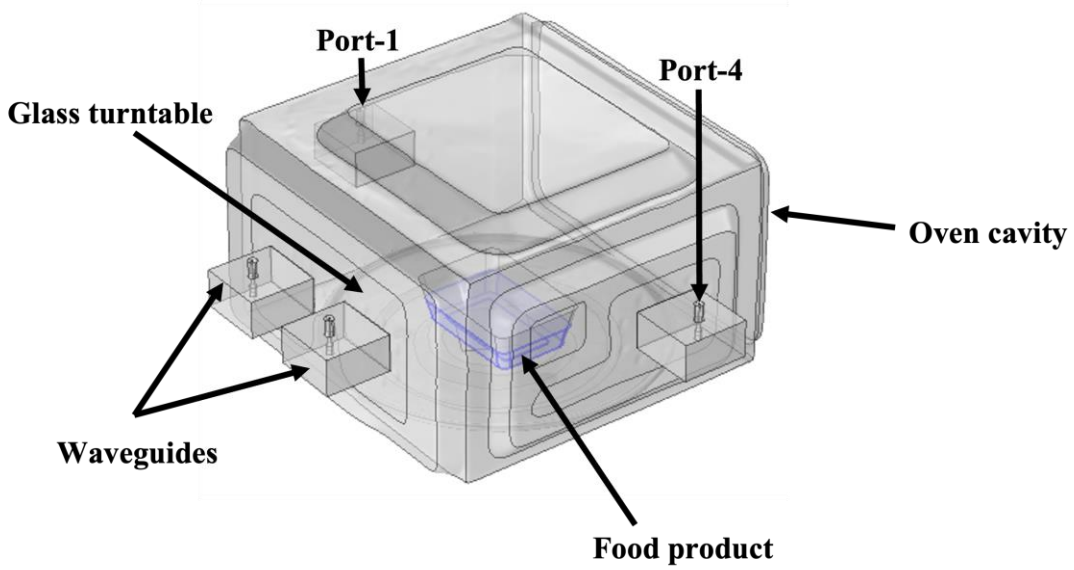

Figure 3.2 A detailed schematic diagram of the multiple-port microwave oven cavity.

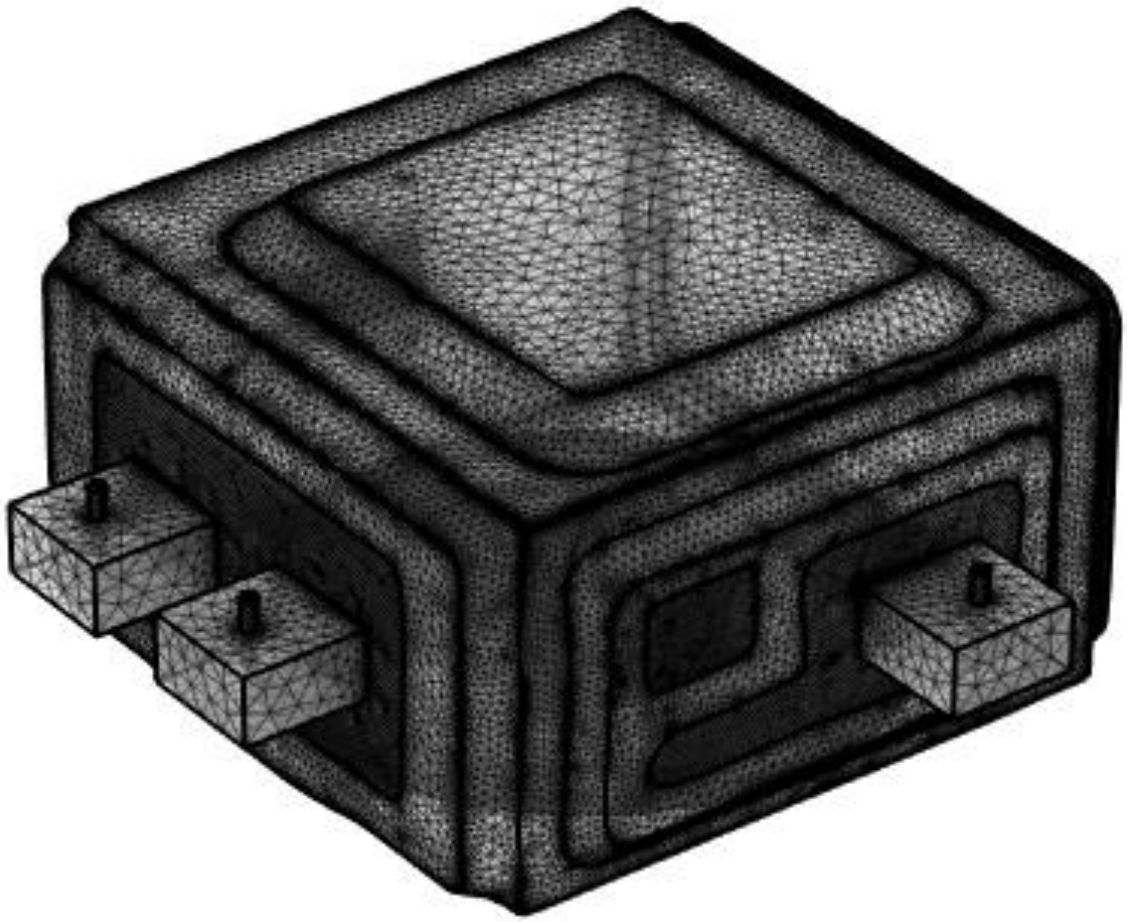

Figure 3.3 Generated mesh of the modeled geometry of the 3-D scanned microwave oven system.

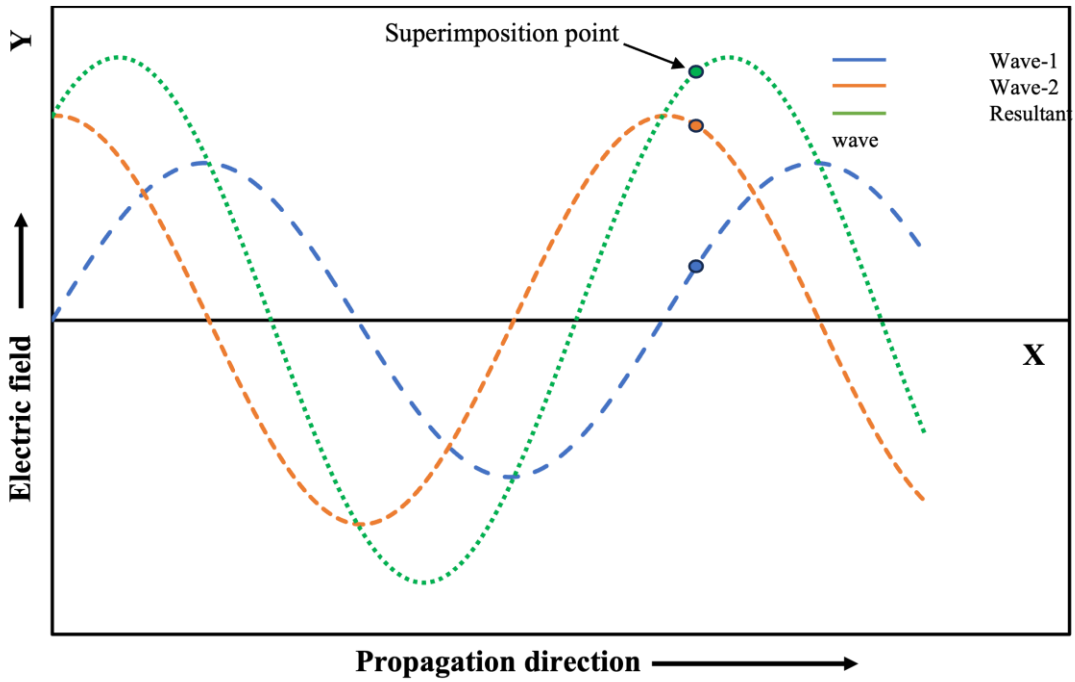

Figure 3.4 Illustration of a resultant wave superimposed by two plane waves with same frequency and a relative phase difference.

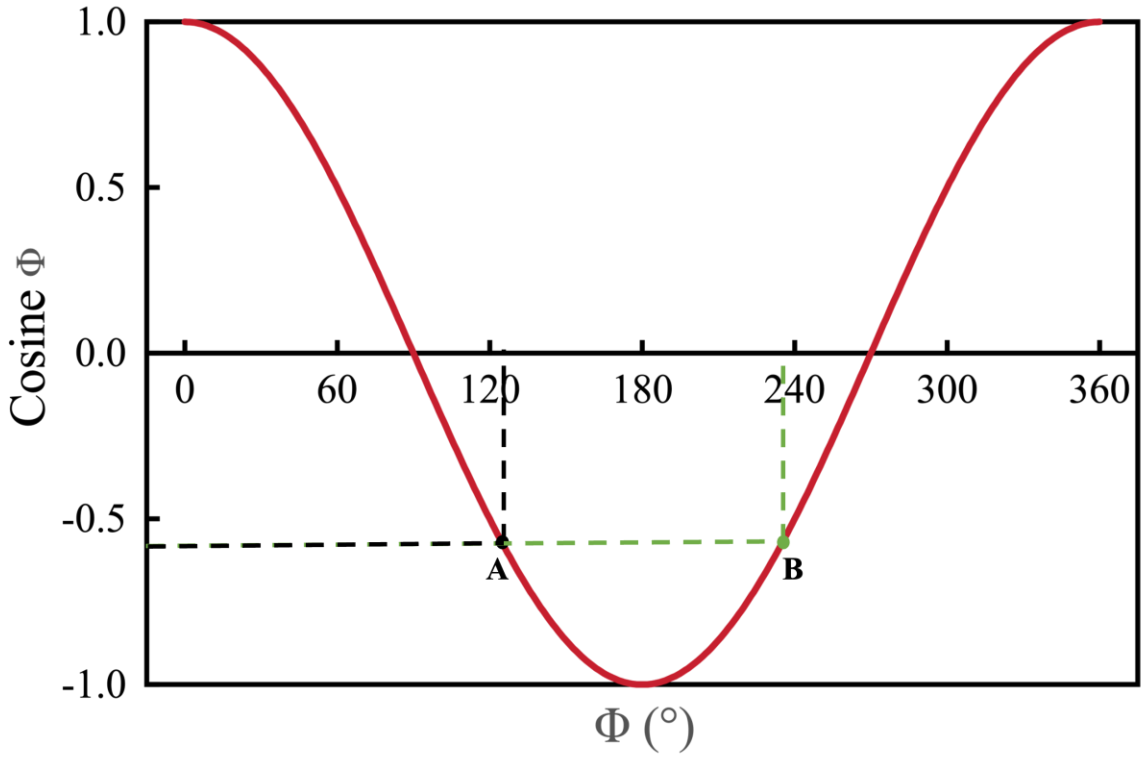

Figure 3.5 Depiction of the movement of a wave through a medium and representation of two points, A and B, having an identical value for the cosine of an angle.

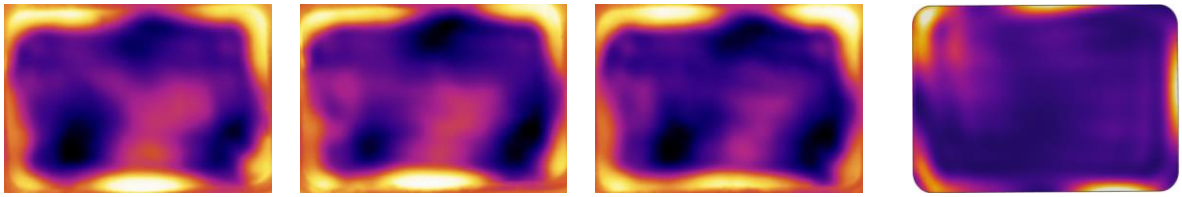

(A) Three replications of experimental thermal profiles

(B) Simulated dissipated power density

Figure 3.6 Comparison of the (A) experimental spatial heating pattern of the mashed potato for three different replications with the (B) simulated power dissipation density of two multiple ports working simultaneously at a relative source phase difference of 0°.

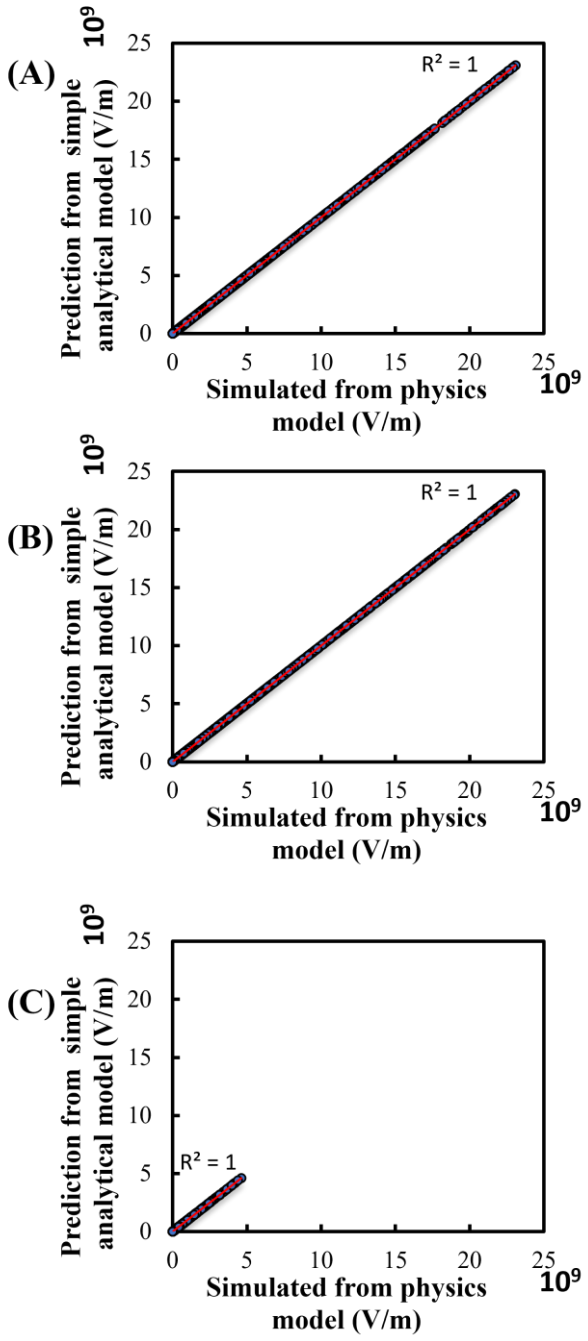

Figure 3.7 Correlation of the electric field between simple analytical model and physics-based model at (A) x-direction, (B) y-direction, and (C) z-direction at an arbitrary relative source phase difference of 135°.

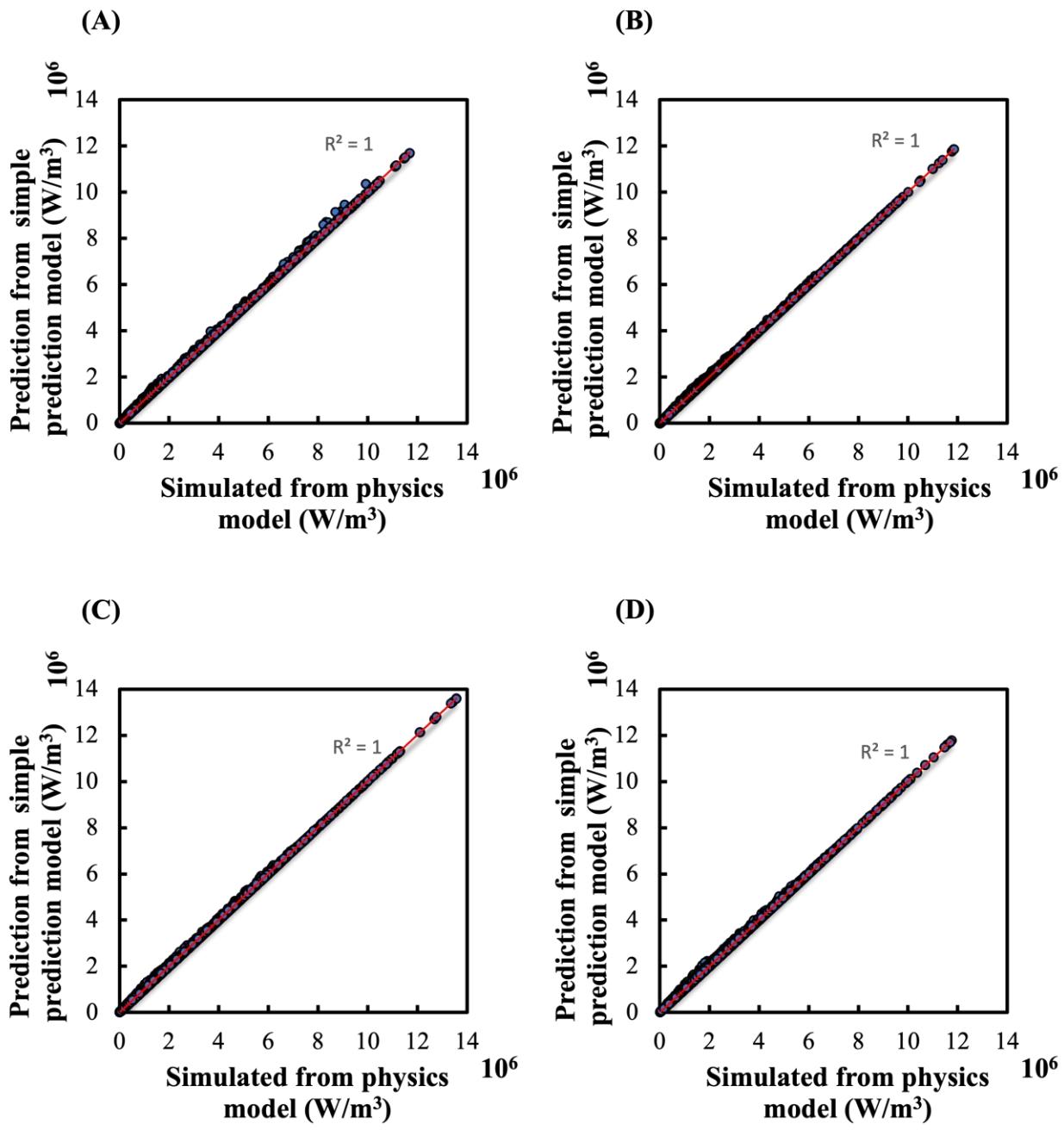

Figure 3.8 Correlation of power dissipation density at arbitrary relative phase of (A) 37°, (B) 135°, (C) 180°, and (D) 223° between simple analytical and physics-based models.

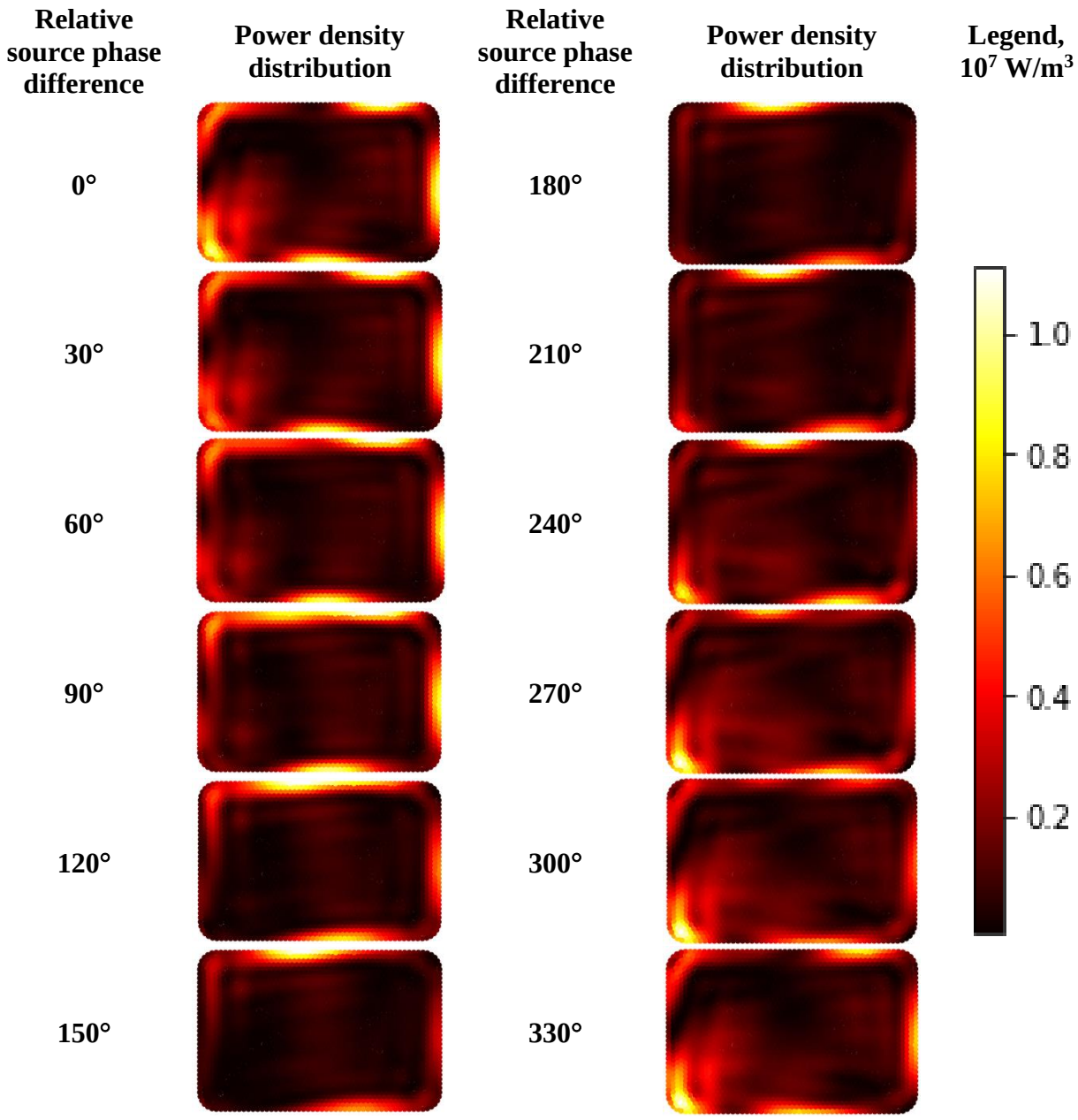

Figure 3.9 The effect of relative source phase difference on the predicted heating pattern using simple analytical model for the top layer of the food product.

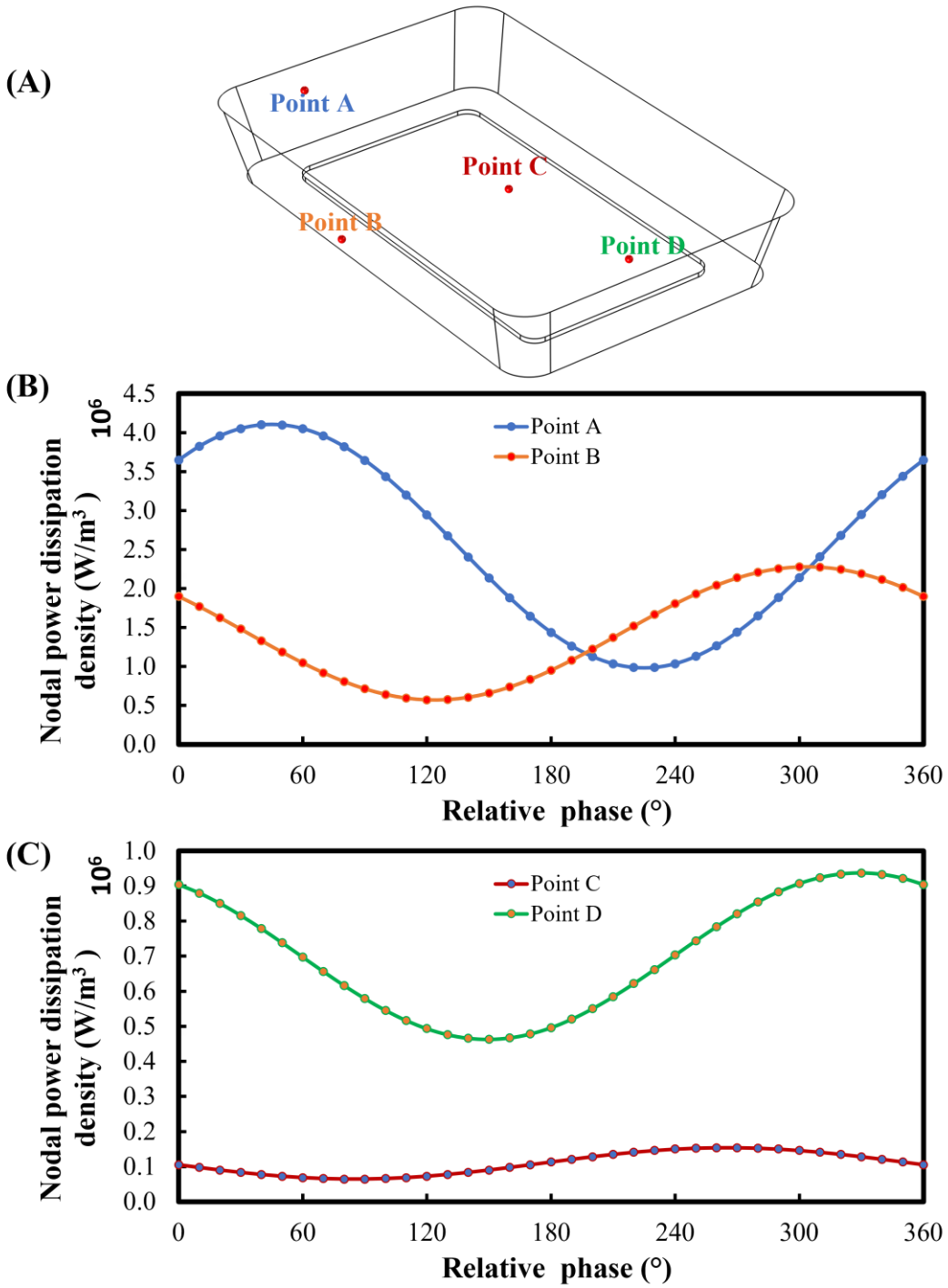

Figure 3.10 Location of the four arbitrary nodal points (A) in the food product and their relative phase-dependent microwave power dissipation densities at edge (B) and center (C) locations.

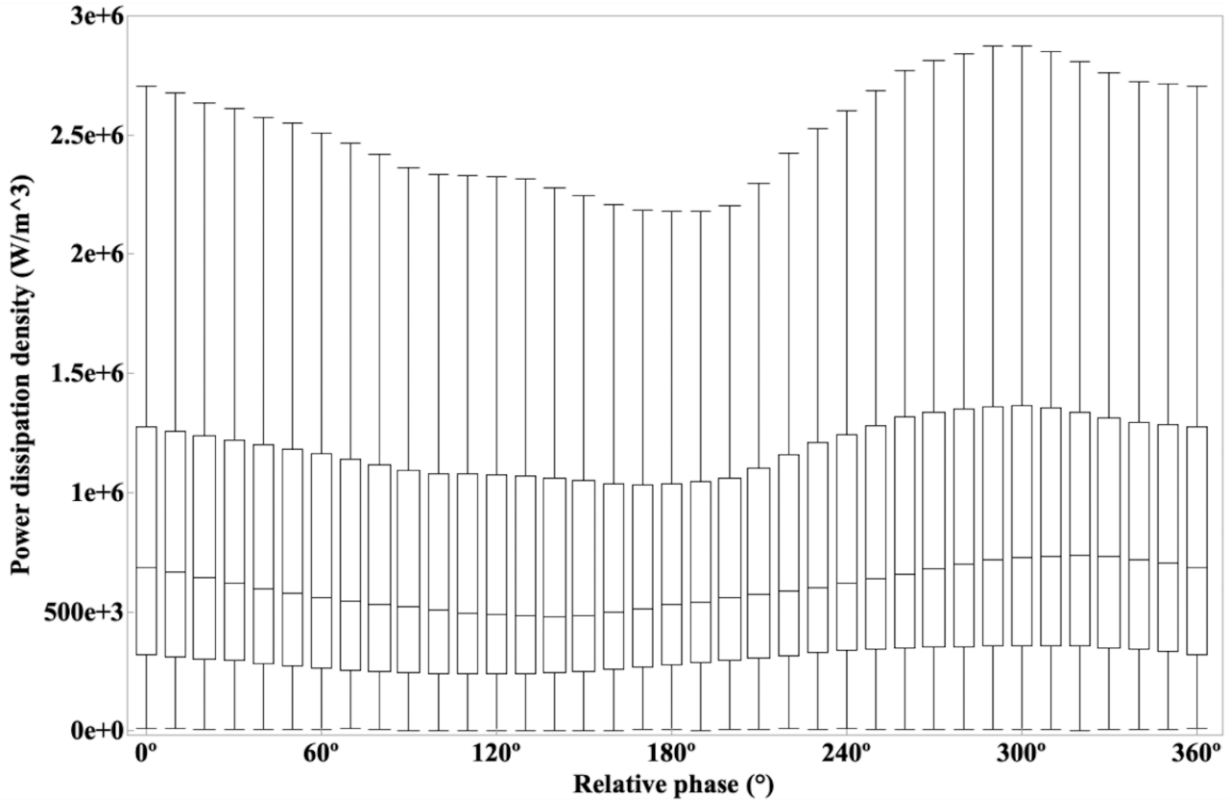

Figure 3.11 Box plot showcasing the effect of relative source phase difference on the power dissipation density.

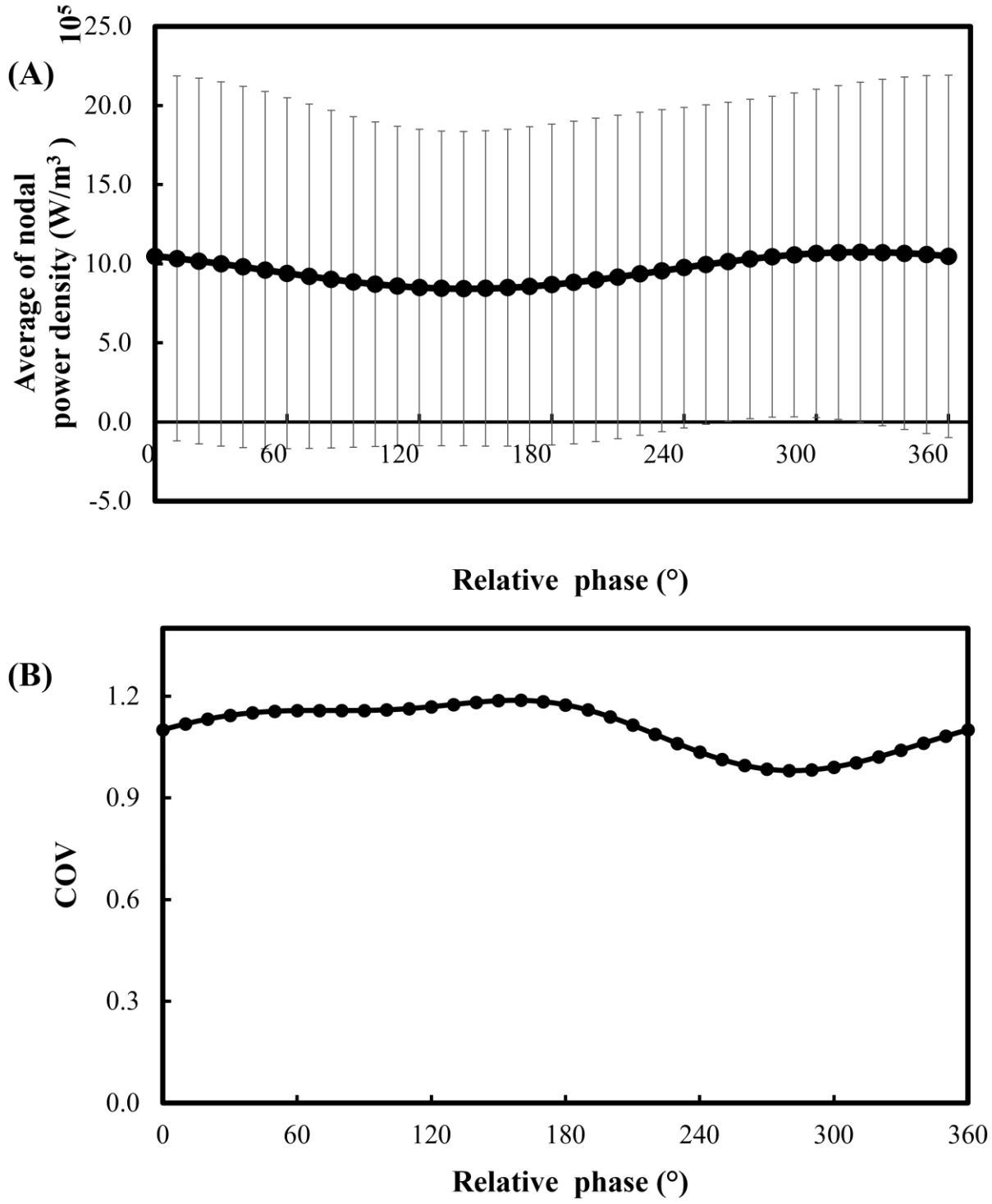

Figure 3.12 The effect of relative source phase difference on (A) average and standard deviation and (B) COV of the nodal power dissipation density.

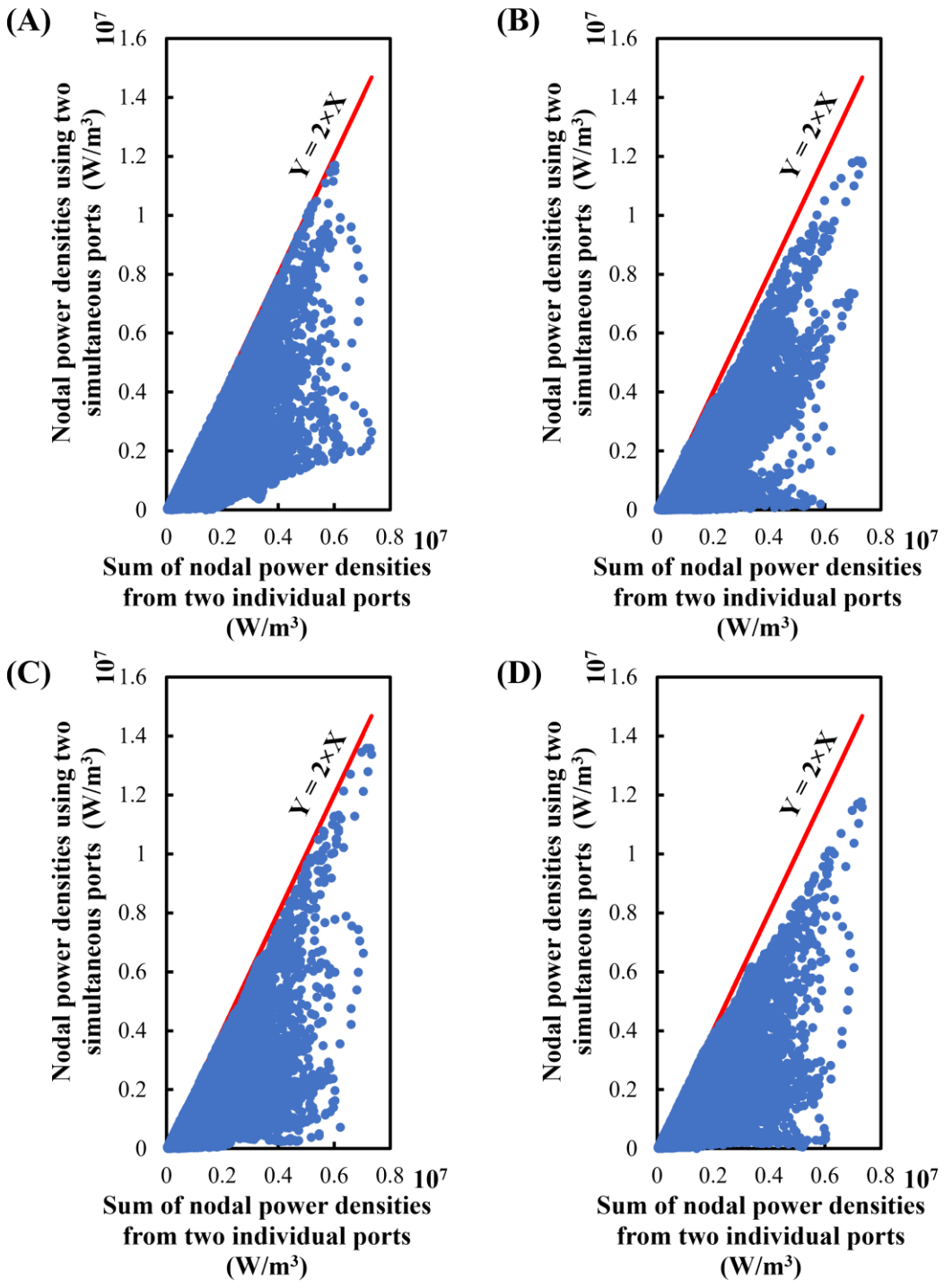

Figure 3.13 Comparison of the nodal power densities within the food product between scenarios of two ports simultaneously working together and sum of the two ports working individually at arbitrary relative phase of (A) 37°, (B) 135°, (C) 180°, and (D) 223°

CHAPTER IV: CONCLUSIONS AND FUTURE WORKS

4.1 Conclusions

In this thesis, multiphysics models were developed in the COMSOL Multiphysics v6.0 (COMSOL Inc., Boston, MA) software to simulate the microwave heating process in a multi-port solid-state microwave system. The validated model was used to understand the multiple port interaction in the multi-port solid-state microwave system and investigate the impact of geometric details on the modeling accuracy. The results demonstrated that the major and minor protrusions in the oven cavity play a crucial role in accurately predicting the locations of hot and cold spots and temperature distribution in the food product. To improve the modeling accuracy, a 3-D scanning approach was utilized to obtain a more precise geometry of the oven cavity and turntable, which improved the prediction accuracy of the developed model as compared to the simple box geometry and manual measurements. Quantitative comparison between the simulated and experimental temperature profiles using the RMSE values along with the often-used qualitative validation further validated the effectiveness of the 3-D scanned geometry in enhancing the modeling accuracy as compared to the other geometries. The use of 3-D scanned geometry yielded a considerable improvement in modeling accuracy when compared to both the simple box geometry and manually measured geometry in a wide range of scenarios involving multiple frequencies and port locations. Although the increased mesh may lead to extended modeling time, the convenience of 3-D scanned technology greatly assists modelers in accurately capturing irregular geometries. Furthermore, the quantitative approach employed for comparing spatial temperature profiles between simulations and experiments serves as a robust method for validating the developed models.

The validated model was used to understand the multiple port interaction and the impact of relative source phase differences on multiple-port interactions in a multi-source solid-state microwave system. An analytical model based on four physics-based modeling was developed to analyze microwave interactions and their effects on power density distribution. The analytical model exactly matched the physics-based modeling results, and extensive characterization of the power density distribution revealed nonuniform patterns and variations in the average and standard deviation of nodal power densities with respect to relative source phase differences.

The findings emphasize the importance of selecting proper relative phases to ensure heating efficiency, uniformity, and selective heating in the microwave system. The constructive and destructive effects of multi-source waves were identified as the main contributors to variations in nodal microwave power densities at different nodal points which further may influence the heating uniformity. Leveraging the relative phase-dependent heating patterns, strategies for relative phase control can be developed to optimize heating performance with a balance between efficiency and uniformity.

Moreover, the developed analytical model provided a means to predict power dissipation density at different relative source phase differences, allowing for a comprehensive understanding and characterization of this effect. The distribution of electric field density and power dissipation density within the food product and oven cavity facilitated selective heating, while the efficiency of calculating these values was addressed by the efficient solution provided by the simple analytical model.

Overall, this study contributes to the field of microwave heating by enhancing the modeling accuracy through 3-D scanned geometries and validating the models using a quantitative comparison approach. Additionally, the investigation of relative source phase differences provides insights into optimizing heating efficiency and uniformity in multi-source microwave systems, with the analytical model offering an efficient and time saving solution for predicting power dissipation density in the food product and oven cavity. These findings have implications for improving microwave heating processes and facilitating better control strategies for enhanced performance in future applications.

4.2 Future Works

In this study, multiphysics-based models based on the 3-D scanning approach and simple analytic models based on limited physics-based modeling results were developed and validated to simulate the dual-port solid-state microwave heating process. Future research can utilize the developed approach and models to study further the multi-port interactions within the solid-state microwave oven cavities.

First, leveraging 3-D scanning technology can facilitate the capture of irregular geometries for improved modeling accuracy. The developed 3-D scanning approach can be used extensively to characterize the geometries of oven cavities from different brands and models. The oven geometries can be compiled as an oven cavity database for food developers to evaluate the effect of oven cavity design on the heating performance of their designed food products. The application of the 3-D scanning approach can also extend to the design of food containers.

Besides, with the validated physics-based and analytical models, future work should study how to incorporate multiple microwave sources for phase and frequency shifting strategies to improve

microwave heating uniformity and power absorption efficiency. This thesis only evaluated dual-port interactions with the same input power from two ports in the solid-state microwave system. A similar analytical approach can be developed for multiple ports (i.e., more than two ports) with different microwave power inputs. With the possibility of generating a large amount of dataset of microwave heating performance from the modeling tools, machine learning algorithms can be employed to define strategies for selective heating based on constructive and destructive interference.

To market the solid-state technology-based microwave ovens, advanced algorithms based on relative phase, power, and frequency can be developed for multiple ports, catering to both refrigerated and frozen samples. To facilitate the industry-wide adoption of solid-state microwave ovens, advancements in semiconductor technology are necessary to reduce costs. Additionally, increasing the power output of solid-state generators is crucial, as the current output is comparatively lower than that of magnetrons.

In summary, the future of solid-state microwave technology involves further research into optimizing microwave heating performance, exploring multiple-port systems, developing advanced algorithms for selective heating, addressing price and power limitations, and expanding the range of food products considered in the models. Advancements in semiconductor technology will play a vital role in driving the adoption of solid-state technology within the industry.

VITA

Kartik Verma was born in Mohali, Punjab, India. He graduated with a Bachelor of Engineering in Food Technology from Panjab University, Chandigarh, India, in 2020. After completing his undergraduate program, he joined the Department of Food Science at the University of Tennessee, Knoxville, to pursue a Master of Science degree under the guidance of Dr. Jiajia Chen and Dr. Hao Gan. His research area mainly focuses on the Multiphysics modeling of the solid-state microwave oven and understanding the multiple-port interaction of solid-state microwave system to improve the uniformity of the microwave heating process.